Influence of Molecular Weight Distribution on the Linear Viscoelastic Properties of Polymer Blends

CHANG DAE HAN, *Department of Chemical Engineering and Polymer Research Institute, Polytechnic University, Brooklyn, New York 11201*

Synopsis

Literature data for the dynamic viscoelastic properties of binary blends of nearly monodisperse polybutadienes, polystyrenes, and poly(methyl methacrylate)s was analyzed using *logarithmic* plots of dynamic storage modulus G' versus loss modulus G'', based on a recent theoretical study by Han and Jhon.[28] It has been found that for binary blends of monodisperse polymers with molecular weights M much greater than the entanglement molecular weight M_e, the value of G' in $\log G'$–$\log G''$ plots becomes independent of molecular weight, increases sharply as small amounts of a high-molecular-weight component are added to a low-molecular-weight component, and passes through a maximum G'_{max} at a critical blend composition $(\phi_2)_{max}$, and that G'_{max} becomes larger and $(\phi_2)_{max}$ becomes smaller as the ratio of component molecular weights increases. However, as the molecular weight distribution of the constituent components becomes broader, the effect of blend composition on G' in $\log G'$–$\log G''$ plots becomes less pronounced. This observation has enabled us to explain why $\log G'$–$\log G''$ plots of binary blends of commercial polymers, namely, blends of two low-density polyethylenes, blends of poly(ϵ-caprolactone) and poly(styrene-*co*-acrylonitrile), and blends of poly(methyl methacrylate) and poly(vinylidene fluoride), all having broad molecular weight distributions, give rise to values of G' between those of the constituent components. When one of the constituent components has molecular weight smaller than M_e, while the other has molecular weight larger, and as small amounts of the high-molecular-weight component are added to the low-molecular-weight component, $\log G'$–$\log G''$ plots of binary blends give rise to values of G' larger than those of the constituent components at low values of G'', but approaches the value of G' for the low-molecular-weight component as the value of G'' is increased. However, as the amount of the high-molecular-weight component is increased above a certain critical composition, binary blends give rise to values of G' close to that of the high-molecular-weight component at all values of G''. The experimentally observed dependence of G' on blend composition in $\log G'$–$\log G''$ plots is favorably compared to the theoretical prediction of a blending law proposed by Montfort and co-workers.[14,15]

INTRODUCTION

During the past two decades, continuing efforts by a number of investigators[1-24] have been spent on enhancing our understanding of the effect of molecular weight distribution on the viscoelastic properties of binary blends of monodisperse homopolymers. Some investigators[1-3,6,7,9-11,14,15] have developed empirical or semiempirical formulas, while others[8,12,16,18,23] have taken a theoretical approach, enabling us to predict with varying degrees of success, the zero-shear viscosity (η_0) and/or steady-state recoverable shear compliance J_e^o of binary blends.

In recent years, we have begun to investigate the dynamic viscoelastic properties (namely, storage and loss moduli, G' and G'') of binary blends of

Journal of Applied Polymer Science, Vol. 35, 167–213 (1988)
 CCC 0021-8995/88/010167-47$04.00

commercial homopolymers having the same chemical structure, but different molecular weight distributions, and binary blends of compatible polymers with dissimilar chemical structures.[25,26] Specifically, we have investigated: (a) blends of two low-density polyethylenes (LDPE) having different molecular weight distributions; (b) blends of poly(methyl methacrylate) (PMMA) and poly(vinylidene fluoride) (PVDF); (c) blends of poly(ε-caprolactone) (PCL) and poly(styrene-*co*-acrylonitrile) (SAN); and (d) blends of PMMA and SAN. Invariably, all commercial polymers have very broad molecular weight distribution. Note that the blend systems consisting of two dissimilar polymers, listed above, are known to be compatible.

In the present paper, we will discuss the dynamic viscoelastic properties, measured in our laboratory, of binary blends of commercial polymers. In interpreting our experimental results for the blend systems, we employed *logarithmic* plots of G' versus G'', which had previously been introduced to investigate the rheological behavior of homopolymers in the molten state.[27,28] In order to facilitate our discussion, we will first review literature data, by recasting them into *logarithmic* plots of G' versus G'', for binary blends of nearly monodisperse components: specifically, binary blends of polybutadienes of Struglinski and Graessley,[22] binary blends of polystyrenes of Montfort et al.,[17] and Kotaka and co-workers,[19,20] respectively, and binary blends of poly(methyl methacrylate)s of Onogi et al.[7] We will then attempt to predict the dependence of G' on blend composition in $\log G'$–$\log G''$ plots, using a blending law proposed by Montfort and co-workers.[14,15] Finally, we will discuss the advantages of using $\log G'$–$\log G''$ plots over $\log G'$–$\log \omega$ and $\log G''$–$\log \omega$ plots, in the investigation of the effect of molecular weight distribution on the linear viscoelastic properties of polymer blends.

PREVIOUS STUDIES ON BLENDING LAW

The important dynamic viscoelastic properties in the terminal region are zero-shear viscosity η_o and steady-state recoverable shear compliance J_e^o,

$$\eta_o = \lim_{\omega \to 0} \frac{G''(\omega)}{\omega} \tag{1}$$

$$J_e^o = \lim_{\omega \to 0} \frac{G'(\omega)}{|G^*(\omega)|^2} \tag{2}$$

where $G^*(\omega)$ is the complex modulus. Note that values of η_o and J_e^o are constant for a given polymer, and are dependent upon molecular weight, molecular weight distribution, and the degree of long-chain branching.

A number of investigators[1-24] have determined experimentally values of η_o and/or J_e^o for binary blends of nearly monodisperse polymers of similar chemical structure (e.g., polybutadiene, polyisobutylene, poly(methyl methacrylate), polystyrene) and attempted to obtain blending laws or to test existing blending laws. In order to facilitate our discussion later, we will review very briefly the highlights of various blending laws proposed in the literature, to the extent that they are relevant to the main idea that we shall expound below.

Assuming that the relaxation spectrum of a binary blend may be represented by the linear superposition of the relaxation spectra of the constituent components, Ninomiya and co-workers[1-3] have proposed a linear blending law for predicting the zero-shear viscosity of blends η_{ob} and steady-state recoverable shear compliance of blends J^o_{eb}:

$$\eta_{ob} = \phi_1\lambda_1\eta_{o1} + \phi_2\lambda_2\eta_{o2} \tag{3}$$

$$J^o_{eb} = \left[\phi_1\lambda_1^2\eta_{o1}^2 J^o_{e1} + \phi_2\lambda_2^2\eta_{o2}^2 J^o_{e2}\right]/\eta_{ob}^2 \tag{4}$$

where η_{oi} denotes zero-shear viscosity of i-th component, J^o_{ei} denotes steady-state recoverable shear compliance of i-th component, ϕ_i denotes the volume fraction (or weight fraction if their densities are identical) of the i-th component, and λ_i is the shift factor of the i-th component, which depends on both the combination and the volume fractions of the constituent components. Hereafter, ϕ_i will be used to designate either volume or weight fraction, whichever is more appropriate at the time.

For undiluted polymers with molecular weights M smaller than a critical value M_c, to which the Rouse theory is applicable, Eq. (4) may be rewritten as[29]

$$J^o_{eb} = \phi_1 J^o_{e1}\left(M_1/\overline{M}_w\right)^2 + \phi_2 J^o_{e2}\left(M_2/\overline{M}_w\right)^2 \tag{5}$$

where M_1 and M_2 are the molecular weights of components 1 and 2, respectively, and $\overline{M}_w$ is the average molecular weight of a blend defined as

$$\overline{M}_w = \phi_1 M_1 + \phi_2 M_2 \tag{6}$$

It can be shown using Eqs. (3) and (5), that for $M_2 \gg M_1$ and $\phi_2 < \phi_1$, η_{ob} always lies between η_{o1} and η_{o2}, while J^o_{eb} goes through a maximum at a certain critical value of ϕ_2, as shown schematically in Figure 1. Indeed, the dependence of J^o_{eb} on blend composition, depicted in Figure 1, has been observed in a number of experimental investigations.[4-7,9,10,14-18,21,22]

The Rouse theory for a polydisperse binary blend may be expressed as[29]

$$J^o_{eb} = \frac{2}{5\rho RT}\frac{\overline{M}_{z+1}\overline{M}_z}{\overline{M}_w} = \frac{2}{5\rho RT}\frac{\phi_1 M_1^3 + \phi_2 M_2^3}{\left(\phi_1 M_1 + \phi_2 M_2\right)^2} \tag{7}$$

where ρ is the density, R is the universal gas constant, T is the absolute temperature, and $\overline{M}_z$ and $\overline{M}_{z+1}$ are the z-th and $(z+1)$th moments of the molecular weight distribution. Equation (7) indicates that J^o_{eb} is very sensitive to the higher averages of molecular weight.

In situations where component 1 may be taken as a homologous solvent of low molecular weight, the blends can be considered as concentrated solutions. For such a case, $\overline{M}_w$ averaged over polymer and solvent is very close to $\phi_2 M_2$ (i.e., $\overline{M}_w \approx \phi_2 M_2$, unless the solution is extremely dilute), and thus $\overline{M}_z \approx$

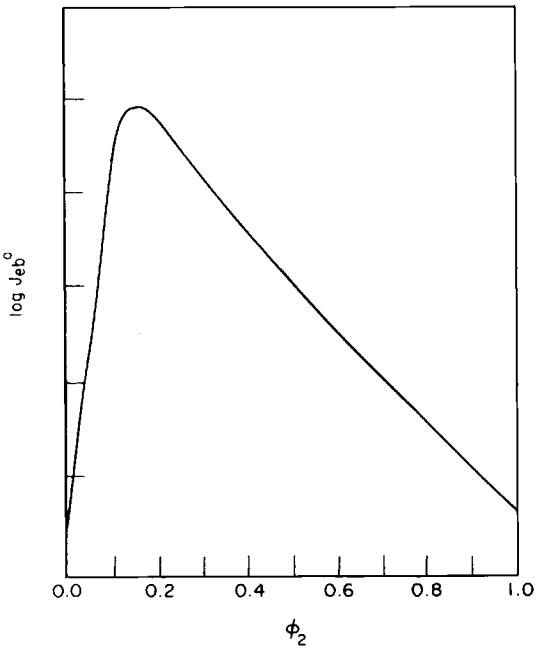

Fig. 1. Schematic describing the dependence of steady-state recoverable compliance J_{eb}^o on blend composition ϕ_2.

$\bar{M}_{z+1} \approx M_2$. Equation (7) then becomes

$$J_{eb}^o = 2M_2/5cRT \tag{8}$$

where c is the concentration (g/cm^3).

Note that Eqs. (3)–(5) would require modification when macromolecules are sufficiently large to have coupling entanglements. In other words, the linear blending law of Ninomiya[1-3] appears to be satisfactory for low-molecular-weight polymers with $M < M_c$, but requires modification for high-molecular-weight polymers whose molecular weight M is greater than the critical entanglement molecular weight for steady-state compliance M_c', above which the J_{eb}^o becomes independent of molecular weight.

Therefore, for polymers with high molecular weight (i.e, $M \gg M_c'$), higher order blending laws have been proposed by assuming, for instance, that the relaxation spectrum of a blend H_b can be represented in quadratic form:[8]

$$H_b(\tau) = \phi_1^2 H_{11}(\tau/\lambda_{11}) + 2\phi_1\phi_2 H_{12}(\tau/\lambda_{12}) + \phi_2^2 H_{22}(\tau/\lambda_{22}) \tag{9}$$

where H_{11} and H_{22} are the relaxation spectra of components 1 and 2, respectively, H_{12} is the cross-relaxation spectrum, and λ_{12} is the empirically determined shift factor. Based on Eq. (9), Bogue et al.[8] obtained the following expressions:

$$\eta_{ob} = K\bar{M}_w^{3.4} \tag{10}$$

$$J_{eb}^o = J_{e1}^o \frac{\left[\phi_1 M_1^2 + \phi_2 M_2^2\right]^2}{\left(\phi_1 M_1 + \phi_2 M_2\right)^4} \tag{11}$$

for binary blends with molecular weights $M_i\,(i = 1,2) > M_c'$. Note that $\overline{M}_w$ in Eq. (10) is the weight-average molecular weight of a blend defined by Eq. (6), and for $M > M_c'$, $J_{e1}^o = J_{e2}^o$ which are independent of molecular weight. It can be shown by Eq. (11) that for $M_2 \gg M_1 > M_c'$ and $\phi_2 < \phi_1$, J_{eb}^o goes through a maximum at a certain critical value of ϕ_2, predicting the behavior depicted in Figure 1.

Assuming a quadratic form of the relaxation spectrum that included four kinds of coupling interactions for binary blends, namely 1-1, 1-2, 2-1, and 2-2 component interactions, Graessley[12] obtained the following expressions

$$\eta_{ob} = \eta_{o1}\left[\phi_1^2 + d_1\phi_1\phi_2 + r\phi_2^2\right] \tag{12}$$

$$J_{eb}^o = J_{e1}^o \frac{\phi_1^2 + d_2\phi_1\phi_2 + r^2\phi_2^2}{\left[\phi_1^2 + d_1\phi_1\phi_2 + r\phi_2^2\right]^2} \tag{13}$$

where r is the ratio of component molecular weights, M_2/M_1, and d_1 and d_2 are molecular structure parameters whose values depend on r. It can be shown by Eq. (13) that J_{eb}^o goes through a maximum at a certain critical value of ϕ_2, behavior depicted schematically in Figure 1.

For monodisperse polymers with molecular weights M greater than M_c, the following expression

$$\eta_o = KM^{3.4} \tag{14}$$

holds and thus substitution of Eqs. (6) and (14) into Eq. (10) gives

$$\eta_{ob} = \left[\phi_1\eta_{o1}^{1/3.4} + \phi_2\eta_{o2}^{1/3.4}\right]^{3.4} \tag{15}$$

Friedman and Porter[11] have reported that Eq. (15) correlates well with the data for binary blends of nearly monodisperse polystyrenes.

Montfort[14] extended the relationship given by Eq. (15) to obtain expressions for the complex viscosity and complex modulus in the terminal region and derived the following expression for J_{eb}^o:

$$J_{eb}^o = J_{e1}^o \frac{1 - \theta - Q\theta}{(1 - \phi_2 + r\phi_2)^{3.4}} \tag{16}$$

where

$$\theta = \frac{r^{3.4/p}}{r^{3.4/p} - 1} \frac{(1 - \phi_2 + r\phi_2)^{3.4/p} - 1}{(1 - \phi_2 + r\phi_2)^{3.4/p}} \tag{17}$$

and

$$Q = \eta_{o1}J_{e1}^o/\eta_{o2}J_{e2}^o \tag{18}$$

in which r is the ratio of component molecular weights, M_2/M_1, and p is an adjustable parameter. Note that for monodisperse components with $M > M_c'$, $J_{e1}^o = J_{e2}^o$ and thus $Q = \eta_{o1}/\eta_{o2}$. Struglinski and Graessley[22] found that Eqs.

(15) and (16) describe very well their experimental data for binary blends of nearly monodisperse polybutadienes.

Very recently, Graessley and Struglinski[23] have developed a blending law on the basis of the tube model of Doi and Edwards,[30] by incorporating constraint release and path length fluctuations in the reptation motion. Montfort et al.[18] also have developed a blending law based on the Doi-Edwards tube model, by considering reptation motion and constraint release.

HAN-JHON THEORY FOR CORRELATING LINEAR VISCOELASTIC PROPERTIES OF MONODISPERSE FLEXIBLE POLYMERS

It is a well-accepted fact today that in oscillatory shear flow the dynamic storage modulus G' may be considered as the amount of energy stored and the dynamic loss modulus G'' as the amount of energy dissipated in a viscoelastic fluid. As suggested by Han and Lem,[27] in oscillatory shear flow one may consider the angular frequency (ω) to be an input variable and G' and G'' output variables (i.e., responses) of the fluid under test. In order to help interpret the experimental results presented below, we will review briefly the theoretical development of Han and Jhon.[28]

Using dimensional analysis, the dimensionless output variables G'_R and G''_R can be represented as functions of the dimensionless input variable $\omega\lambda$ by

$$G'_R = \frac{G'}{G_o} = F_1(\omega\lambda) \tag{19}$$

and

$$G''_R = \frac{G''}{G_o} = F_2(\omega\lambda) \tag{20}$$

where λ is the relaxation time of the fluid and G_o is a quantity that has the dimension of stress.

In oscillatory shear flow of monodisperse linear flexible polymers, on the basis of the Doi-Edwards theory[30] we have the following expressions:

$$G' = \frac{8}{\pi^2} \sum_{p\,\text{odd}} \frac{G_o}{p^2} \frac{(\omega\lambda_p)^2}{1 + (\omega\lambda_p)^2} \tag{21}$$

and

$$G'' = \frac{8}{\pi^2} \sum_{p\,\text{odd}} \frac{G_o}{p^2} \frac{\omega\lambda_p}{1 + (\omega\lambda_p)^2} \tag{22}$$

in which λ_p is the relaxation time spectrum defined as

$$\lambda_p = \lambda_D/p^2;\ p = 1,3,5,\ldots N \tag{23}$$

where λ_D is the disengagement time defined as

$$\lambda_D = L^2/D\pi^2 \tag{24}$$

In Eq. (24), L is an arc length, which is proportional to molecular weight and D is the curvilinear diffusion coefficient, which depends on molecular weight and temperature.

In order to facilitate our analysis here, let us consider the situation of a single relaxation time, that is, $p = 1$ in Eq. (23). In this situation, Eqs. (21) and (22) reduce to

$$G'_M = \frac{(\omega\lambda_D)^2}{1 + (\omega\lambda_D)^2} \tag{25}$$

and

$$G''_M = \frac{\omega\lambda_D}{1 + (\omega\lambda_D)^2} \tag{26}$$

where G'_M and G''_M are dimensionless variables defined by $G'_M = (\pi^2/8)G'/G_o$ and $G''_M = (\pi^2/8)G''/G_o$, respectively. According to Osaki and Doi,[31] for monodisperse polymers with $M > M_e$, G_o in Eqs. (21) and (22) is represented by the plateau modulus, G_N^o,

$$G_o = G_N^o = \rho RT/M_e \tag{27}$$

Note that for a monodisperse polymer with $M < M_e$, G_o in Eqs. (21) and (22) is given by

$$G_o = \rho RT/M \tag{28}$$

By eliminating $\omega\lambda_D$ from Eqs. (25) and (26), we obtain

$$(G'_M)^2 + (G''_M)^2 = G'_M \tag{29}$$

Equation (29) gives the following relationships between G'_M and G''_M:

$$\text{(i) } G'_M = \left(1 - \sqrt{1 - 4(G''_M)^2}\right)/2 \tag{30}$$

and

$$\text{(ii) } G'_M = \left(1 + \sqrt{1 - 4(G''_M)^2}\right)/2 \tag{31}$$

Note that, in order for Eqs. (30) and (31) to have a physical significance, G''_M must be smaller than 0.5. It can easily be shown that this restriction is satisfied in physical systems.

For $\omega\lambda_D \ll 1$, from Eqs. (25) and (26) we have

$$G'_M = (G''_M)^2 \tag{32}$$

Rewriting Eq. (32) in terms of G' and G'', we obtain

$$G' = (\pi^2/8)(G'')^2/G_o \tag{33}$$

Taking logarithms of both sides of Eq. (33), we obtain

$$\log G' = 2\log G'' - \log G_o + \log(\pi^2/8) \tag{34}$$

For monodisperse polymers with $M < M_e$, substitution of Eq. (28) into Eq. (34) gives

$$\log G' = 2\log G'' - \log(\rho RT/M) + \log(\pi^2/8) \tag{35}$$

On the other hand, for monodisperse polymers with $M > M_e$, substitution of Eq. (27) into Eq. (34) gives

$$\log G' = 2\log G'' - \log(\rho RT/M_e) + \log(\pi^2/8) \tag{36}$$

Figure 2 gives a schematic description of the relationship between $\log G'$ and $\log G''$ for linear flexible monodisperse polymers with molecular weight

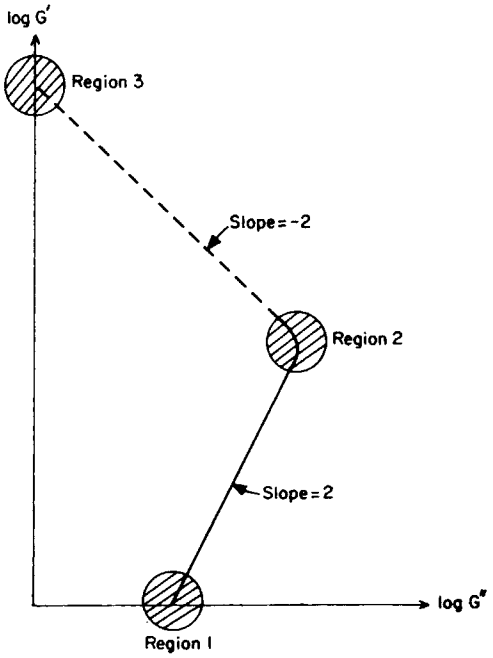

Fig. 2. Schematic describing a relationship between $\log G'$ and $\log G''$ for flexible monodisperse polymers.

(M) greater than the molecular weight between entanglement spacings (M_e). Note in Figure 2 that according to Eqs. (30) and (31), the curve changes its direction at the value $G' = G'' = (4/\pi^2)G_o$.

It is seen in Eq. (35) that for unentangled macromolecules (i.e., $M < M_e$), values of G' depend on molecular weight M and will be shifted downward in the $\log G'$–$\log G''$ plot as M decreases further away from M_e. Note from Eq. (36) that for entangled macromolecules ($M > M_e$), $\log G'$–$\log G''$ plots do not depend on molecular weight and are only a very weak function of temperature. It can be shown from Eq. (36) that an increase in temperature from T_1 to T_2 (in absolute temperature) will shift the value of $\log G'$ by the amount of $\log(T_1/T_2)$. For instance, an increase of temperature from 180 to 240°C will shift the value of $\log G'$ by the amount of 0.054. Such an insignificant amount of shift in $\log G'$ would hardly be noticeable in the $\log G'$–$\log G''$ plots. In other words, $\log G'$–$\log G''$ plots give rise to a correlation that would become *virtually* independent of temperature and, also, independent of molecular weight M for flexible monodisperse polymers with $M > M_e$.

ANALYSIS OF LITERATURE DATA FOR THE LINEAR VISCOELASTIC PROPERTIES OF BINARY BLENDS OF NEARLY MONODISPERSE POLYMERS

In order to help facilitate an analysis of the linear viscoelastic properties of binary blends of commercial polymers determined in our laboratory, we will first analyze the linear viscoelastic properties of binary blends of nearly monodisperse polymers, published in the literature. To minimize any confusion that might arise, in presenting literature data we will use sample codes as they appeared in the original papers.

Binary Blends of Nearly Monodisperse Polybutadienes

Struglinski and Graessley[22] have synthesized various grades of nearly monodisperse linear polybutadienes (PB) by anionic polymerization, then investigated the dynamic viscoelastic properties of binary blends. We will recast their data into *logarithmic* plots of G' against G'' and then discuss the effect of blend composition (i.e., polydispersity) on the linear viscoelastic properties of binary blends. Table I gives information on the molecular weight of three grades of PB, 41L, 174L, and 435L (22). According to Struglinski and Graessley,[22] M_e is 1,859 for undiluted PB. Earlier, Rachefort et al.[32] reported

TABLE I
Molecular Weights of the Polybutadienes Synthesized by Struglinski and Graessley[22]

Sample code	M[a]	$\bar{M}_w/\bar{M}_n$[b]	M[c]
41L	40,700	1.04	39,000
174L	174,000	1.04	181,000
435L	435,000	1.03	450,000

[a] Calculated from intrinsic viscosity in tetrahydrofuran, $[\eta] = 2.27 \times 10^{-4} M^{0.75}$.
[b] Determined with gel permeation chromatography.
[c] Determined with light scattering.

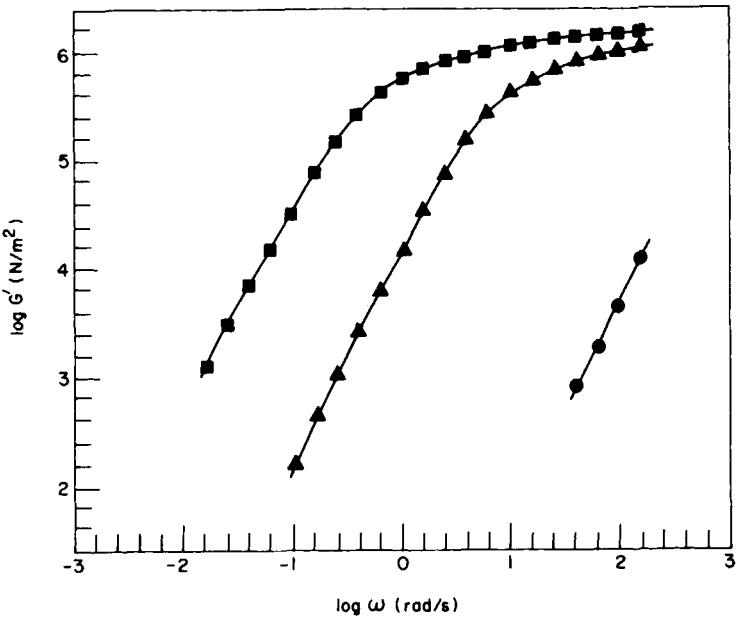

Fig. 3. Log G' vs. log ω for nearly monodisperse linear polybutadienes at 50°C:[21] (●) 41L; (▲) 174L; (■) 435L.

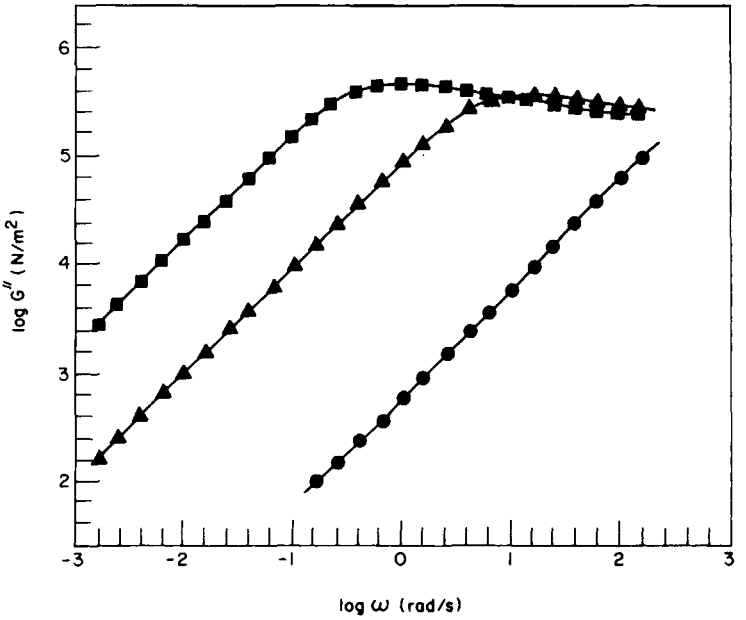

Fig. 4. Log G'' vs. log ω for nearly monodisperse linear polybutadienes at 50°C.[21] Symbols are the same as in Fig. 3.

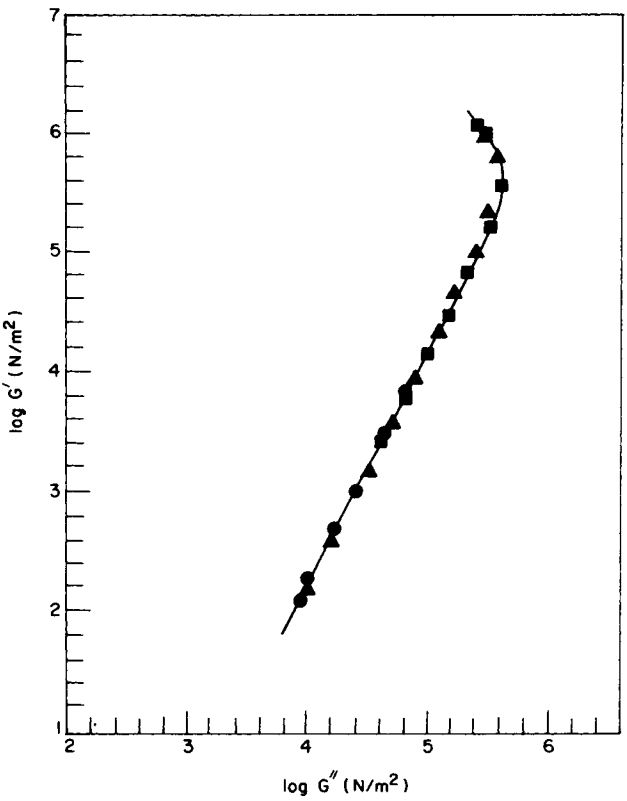

Fig. 5. Log G' vs. log G'' for nearly monodisperse linear polybutadienes at 50°C. Symbols are the same as in Fig. 3.

that $M_e = 1{,}700$, $M_c = 5{,}000$, and $M_c' = 11{,}900$ for undiluted PB. Based on these values, it can be said that the three PBs listed in Table I have molecular weights $M > M_c' \gg M_e$.

Figures 3 and 4 give $\log G'$–$\log \omega$ and $\log G''$–$\log \omega$ plots, respectively, for the three PB samples at 50°C.[21] It is seen in Figures 3 and 4 that values of both G' and G'' increase with molecular weight, until G'' attains a maximum value. However, when the values of $\log G'$ in Figure 3 are plotted against the values of $\log G''$ in Figure 4, we observe that the dependence of G' on molecular weight disappears, as may be seen in Figure 5. This behavior certainly is predicted by Eq. (36). Similar observation was reported earlier by Han and Jhon[28] for other nearly monodisperse polymers.

Figure 6 gives $\log G'$–$\log G''$ plots for PB 41L at three temperatures, 25, 50, and 75°C. Similar plots are given in Figure 7 for PB 174L and in Figure 8 for PB 435L. It is seen in Figures 6 to 8 that the effect of temperature on G' in $\log G'$–$\log G''$ plots is not noticeable at all for PB 41L and PB 174L over the entire range of G'' investigated and, also, for PB 435L until very high values of G'' are reached. It can be said from Figures 6 to 8 that in the terminal region (i.e., Region 1 in Figure 2), $\log G'$–$\log G''$ plots are *virtually* independent of temperature. This experimental observation is also predicted by Eq. (36). Note that an increase in temperature from 25 to 75°C would have shifted

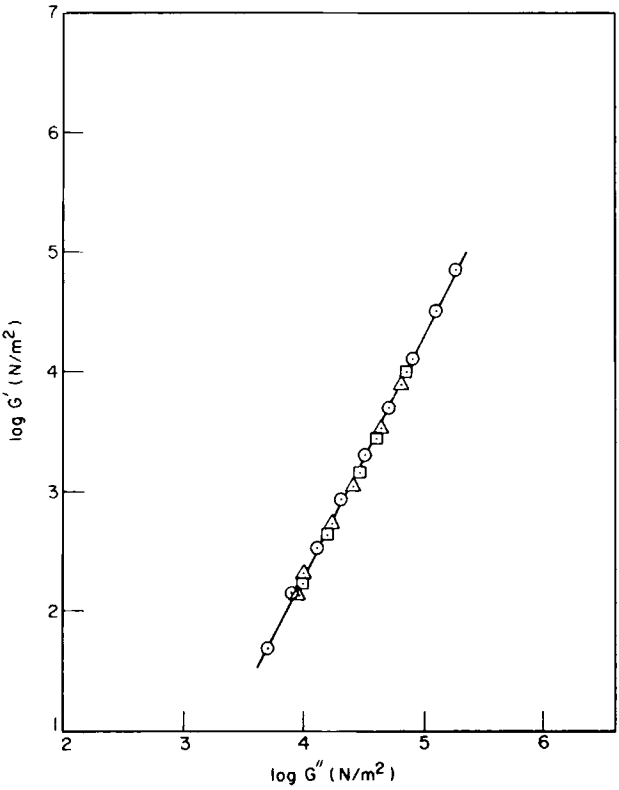

Fig. 6. Log G' vs. log G'' for polybutadiene 41L at temperatures (°C): (⊙) 25; (△) 50; (⊡) 75.

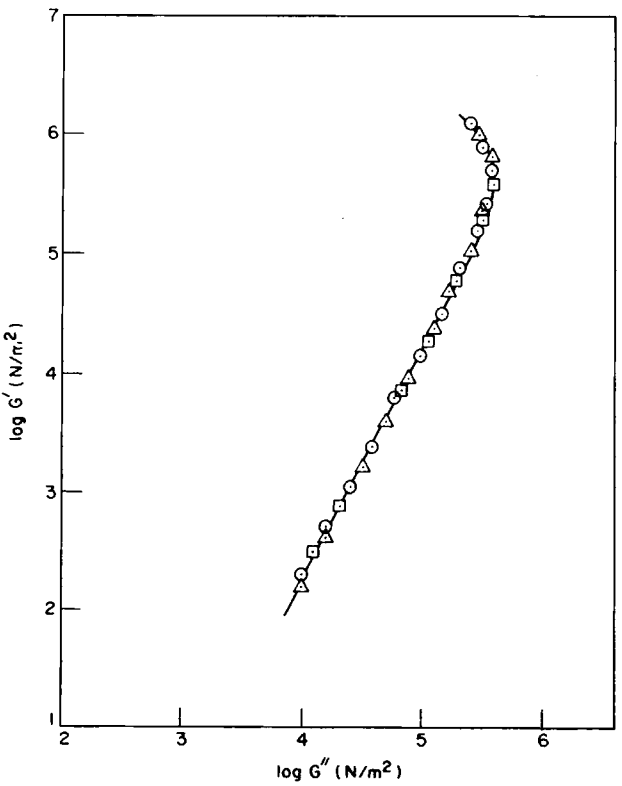

Fig. 7. Log G' vs. log G'' for polybutadiene 174L at temperatures (°C): (⊙) 27; (△) 50; (⊡) 75.

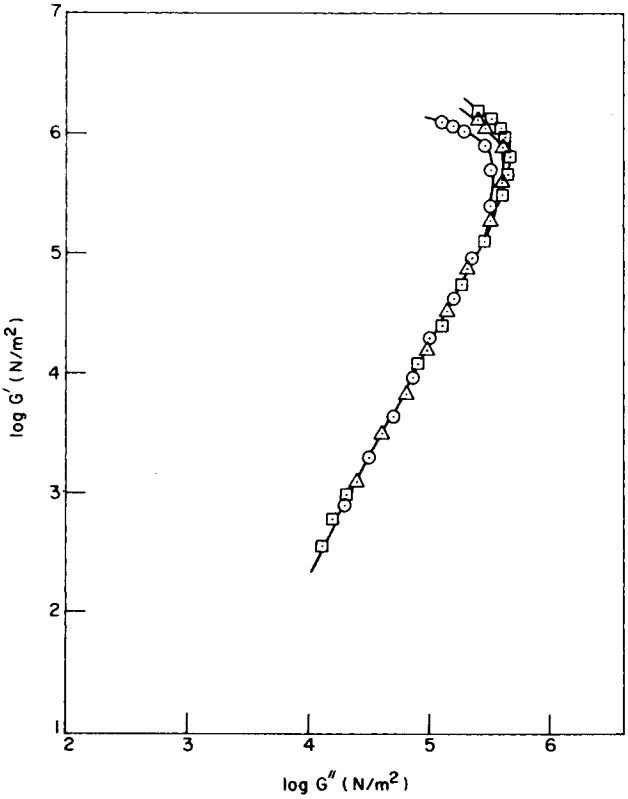

Fig. 8. Log G' vs. log G'' for polybutadiene 435L at temperatures (°C): (⊙) 25; (△) 50; (⊡) 75.

values of log G' by 0.0673 and, within experimental uncertainties, such an insignificant amount of shift in log G' is not noticeable in Figures 6 to 8. Experimental observations similar to those in Figures 6 to 8 have been reported for other polymer systems by Han and co-workers.[25-28,33,34]

It seems appropriate to mention, at this juncture, that in 1941 Cole and Cole[35] first used the *ordinary* coordinate system to plot the real part (ϵ') of the complex dielectric constant on the abscissa against imaginary part (ϵ'') on the ordinate, for a number of polar materials at various temperatures. Since then, Cole-Cole plots have widely been used for interpreting rheological data. It should be pointed out that the Cole-Cole plot falls on a circular arc and a different arc is observed for each temperature, with the shape of the circular arc varying with temperature. However, in view of the fact that log G'–log G'' plots give rise to correlations that become *virtually* independent of temperature and, also, independent of molecular weight M for flexible monodisperse polymers with $M > M_e$, as shown above (see also Refs. 27 and 28), and that one can offer a theoretical interpretation of the log G–log G'' correlations using molecular theories,[28] the log G'–log G'' plot should *not* be considered to be the same as the Cole-Cole plots.

It is seen in Figure 8 that for sample 435L, which has the largest molecular weight of the three samples, the temperature dependence of G' is noticeable at very large values of G''. In view of the fact that sample 435L is not

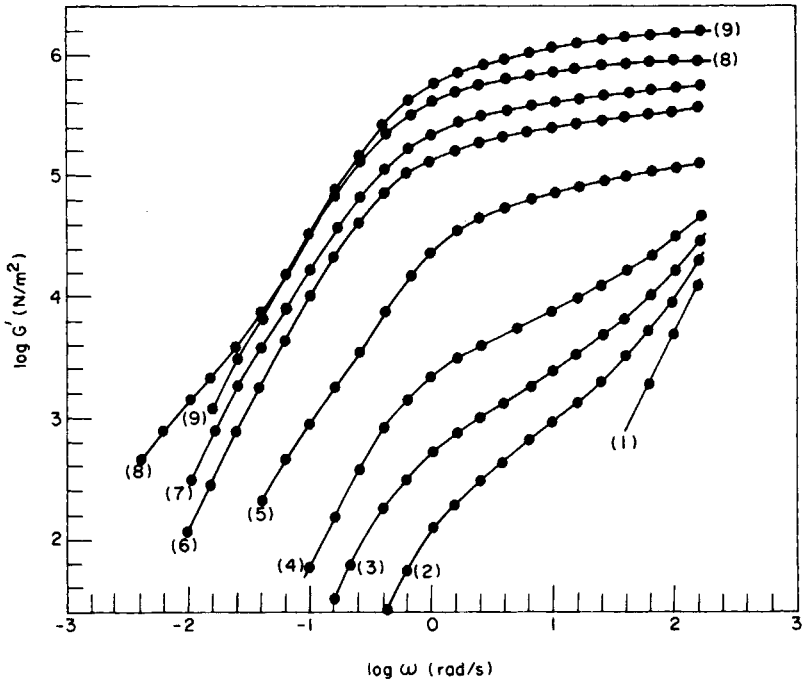

Fig. 9. Log G' vs. log ω for 41L/435L binary blends of polybutadiene at 50°C:[21] (1) 41L; (2) $\phi_2 = 0.025$; (3) $\phi_2 = 0.05$; (4) $\phi_2 = 0.1$; (5) $\phi_2 = 0.36$; (6) $\phi_2 = 0.56$; (7) $\phi_2 = 0.7$; (8) $\phi_2 = 0.9$; (9) 435L.

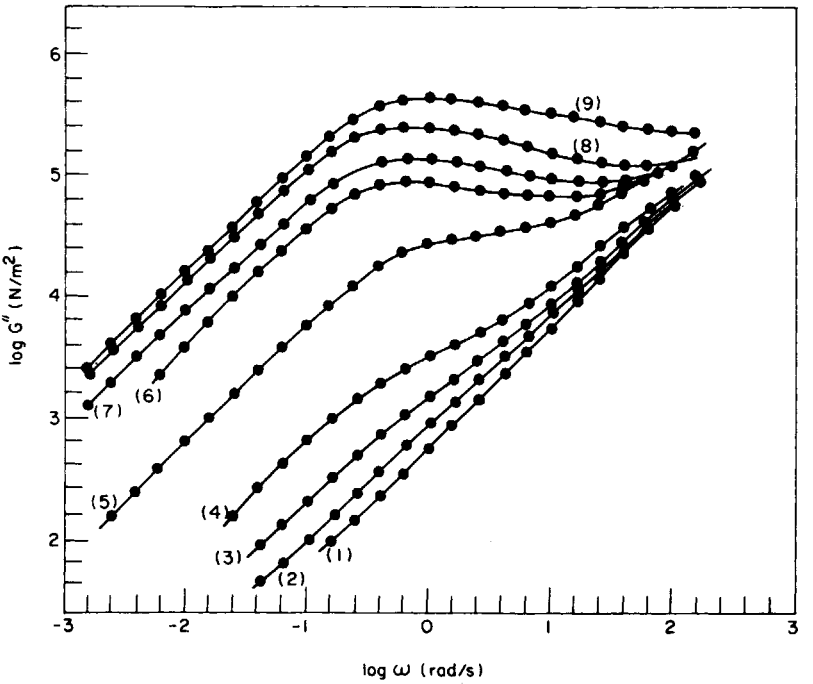

Fig. 10. Log G'' vs. log ω for 41L/435L binary blends of polybutadiene at 50°C.[21] Symbols are the same as in Fig. 9.

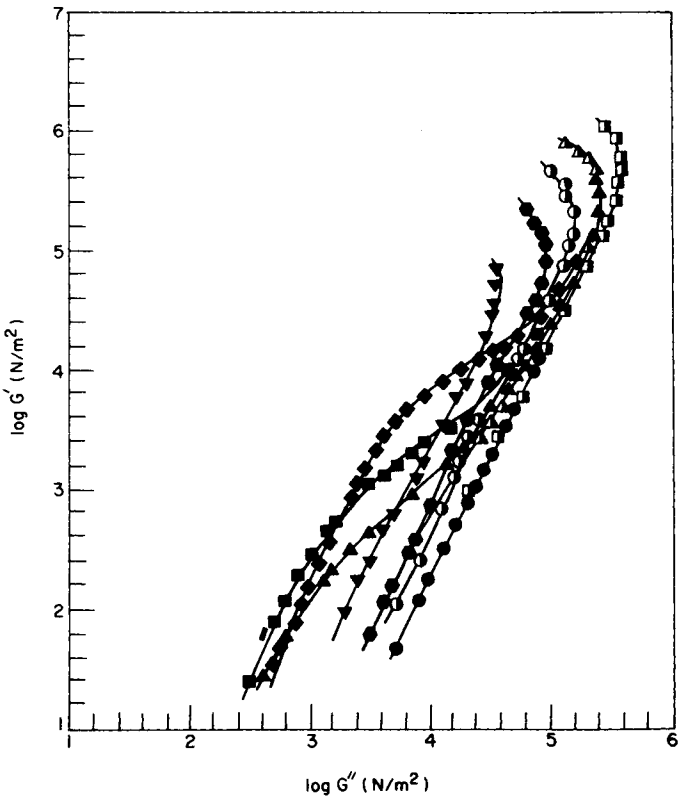

Fig. 11. Log G' vs. log G'' for 41L/435L binary blends of polybutadiene. (●) 41L; (◨) 435L; (▲) $\phi_2 = 0.025$; (■) $\phi_2 = 0.05$; (◆) $\phi_2 = 0.1$; (▼) $\phi_2 = 0.36$; (●) $\phi_2 = 0.56$; (◑) $\phi_2 = 0.7$; (▲) $\phi_2 = 0.9$.

perfectly monodisperse (see Table I), undoubtedly small amounts of low-molecular-weight fractions might have been present in the sample. When sample 435L was subject to high-frequency deformation (i.e., Region 2 in Fig. 2), the Rouse motion of polymer chains between entanglement points may have contributed to relaxation processes in addition to the reptation motion, thus giving rise to temperature dependence in the log G'–log G'' plot. It should be remembered that Eq. (29) was derived on the assumption that relaxation processes are represented by reptation motion only.

Figures 9 and 10 give log G'–log ω and log G''–log ω plots, respectively, for 41L/435L binary blends at 50°C.[21] It is seen in Figures 9 and 10 that values of G' and G'', respectively, for the binary blends lie between those of the constituent components. However, when G' is plotted against G'' on the *logarithmic* scale, as shown in Figure 11, values of G' for all blend samples lie above those of the constituent components. Note in Figure 11 that for a given value of G'', values of G' for the constituent components are the same (see Fig. 5).

It is of interest to observe in Figure 11 that at very low values of G'' (i.e., for $G'' < 10^3$ N/m^2) the value of G' for $\phi_2 = 0.05$ is largest among the blends and then decreases, approaching that of the constituent components as ϕ_2

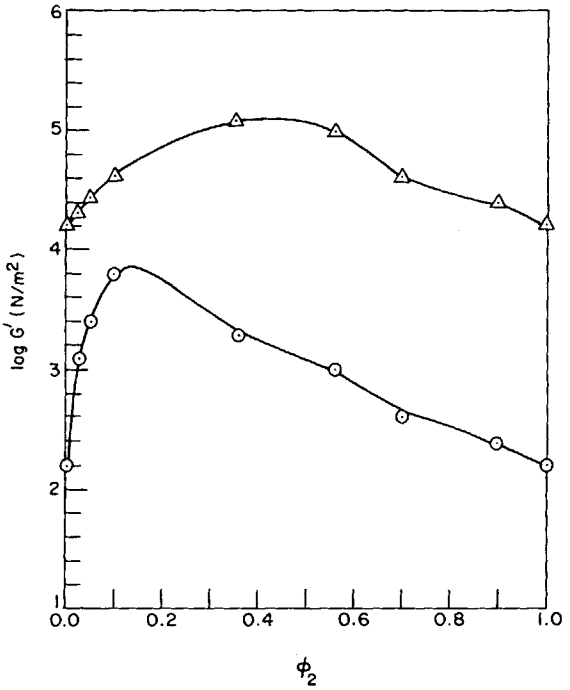

Fig. 12. Log G' vs. ϕ_2 for 41L/435L binary blends of polybutadiene at different values of G'' (N/m^2): (⊙) 10^4; (△) 10^5.

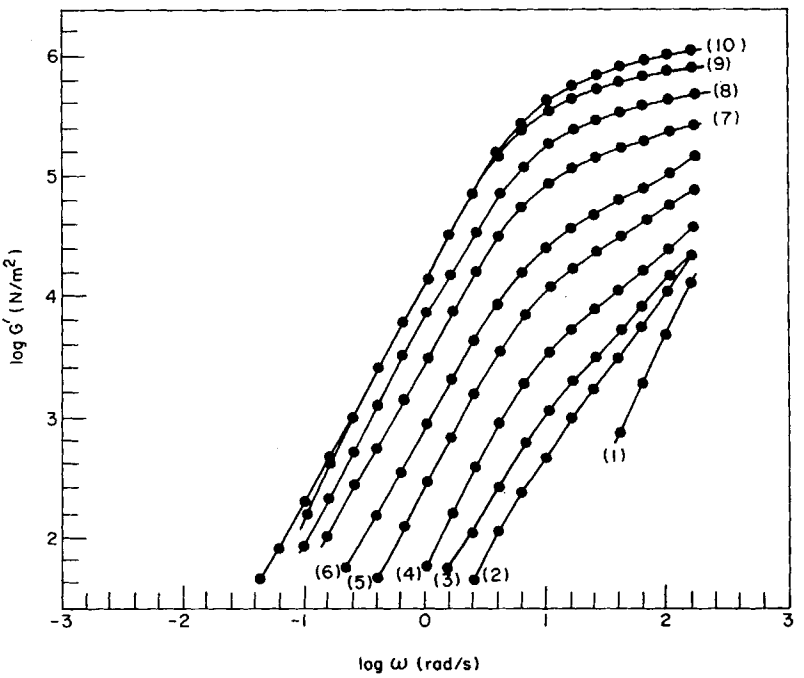

Fig. 13. Log G' vs. log ω for 41L/174L binary blends of polybutadiene at 50°C:[21] (1) 41L; (2) $\phi_2 = 0.025$; (3) $\phi_2 = 0.05$; (4) $\phi_2 = 0.1$; (5) $\phi_2 = 0.2$; (6) $\phi_2 = 0.3$; (7) $\phi_2 = 0.5$; (8) $\phi_2 = 0.7$; (9) $\phi_2 = 0.9$; (10) 174L.

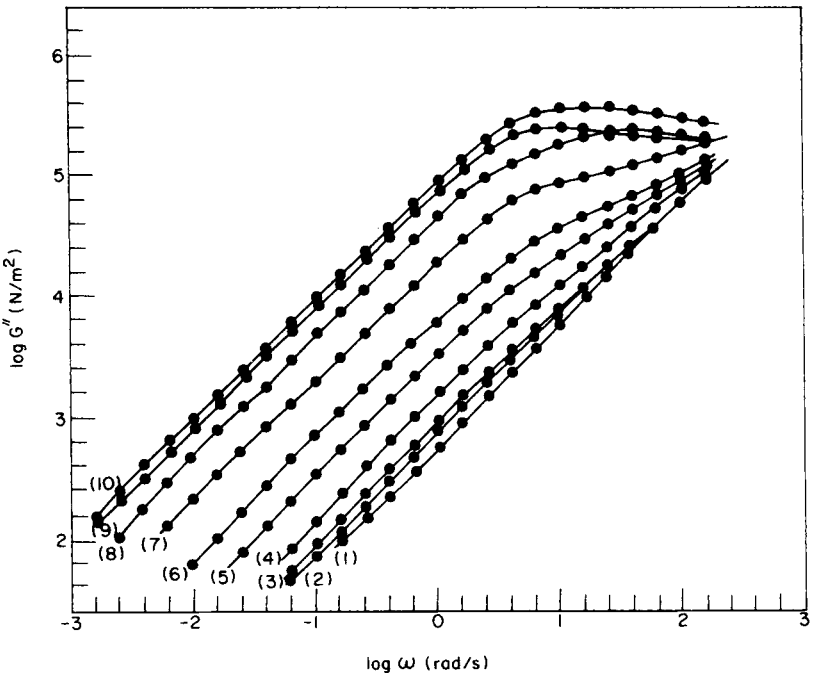

Fig. 14. Log G'' vs. log ω for 41L/174L binary blends of polybutadiene at 50°C.[21] Symbols are the same as in Fig. 13.

approaches 1. In other words, G' goes through a maximum at a certain critical blend composition. This observation is demonstrated at two values of G'' in Figure 12. The dependence of G' on blend composition, observed in Figure 12, is very similar to the dependence of J_{eb}^o on blend composition, that is predicted by various blending laws, namely, Eqs. (4), (11), (13), and (16), and shown schematically in Figure 1. However, there is a very important difference between the two in that, log G'–log G'' plots provide information on the dependence of G' on blend composition in the entire range of G'' investigated, whereas J_{eb}^o cannot since it is obtained in the limit as the angular frequency approaches zero, i.e., $\omega \to 0$ (see Eq. (2) for the definition of J_e^o). Therefore, it can be concluded that log G'–log G'' plots are very useful for investigating the dependence of fluid elasticity on blend composition as a function of G'', i.e., at varying degrees of energy dissipated.

It is seen in Figure 11 that the dependence of G' on blend composition becomes more complicated as G'' increases. For instance, at very low concentrations ($\phi_2 < 0.1$) and at very high concentrations ($\phi_2 > 0.8$), values of G' approach those of the constituent components at large values of G''. On the other hand, at intermediate concentrations ($0.1 < \phi_2 < 0.8$), values of G' for the 41L/435L binary blends in log G'–log G'' plots are greater than those of the constituent components over the entire range of G'' investigated. The dependence of G' on blend composition over a wide range of G'' can be predicted using a blending law. Presented below are results by a blending law.

Figures 13 and 14 give log G'–log ω and log G''–log ω plots, respectively, for 41L/174L binary blends at 50°C.[21] Again, over the entire range of ω investi-

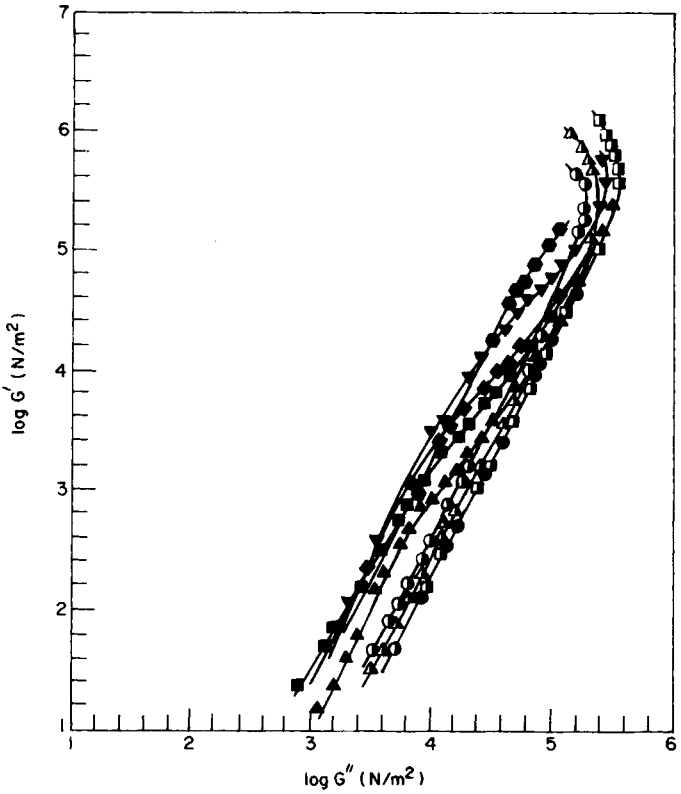

Fig. 15. Log G' vs. log G'' for 41L/174L binary blends of polybutadiene. (●) 41L; (◨) 174L; (▲) $\phi_2 = 0.025$; (■) $\phi_2 = 0.05$; (◆) $\phi_2 = 0.1$; (▼) $\phi_2 = 0.2$; (⬣) $\phi_2 = 0.3$; (◑) $\phi_2 = 0.7$; (▲) $\phi_2 = 0.9$.

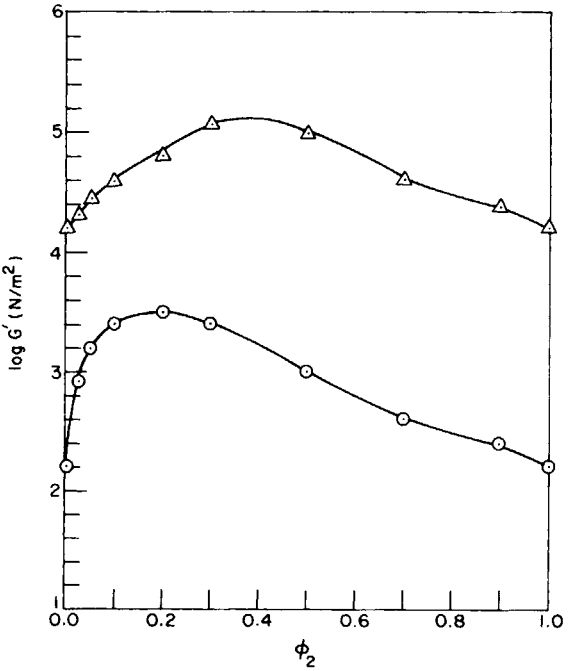

Fig. 16. Log G' vs. ϕ_2 for 41L/174L binary blends of polybutadiene at different values of G'' (N/m^2): (⊙) 10^4; (△) 10^5.

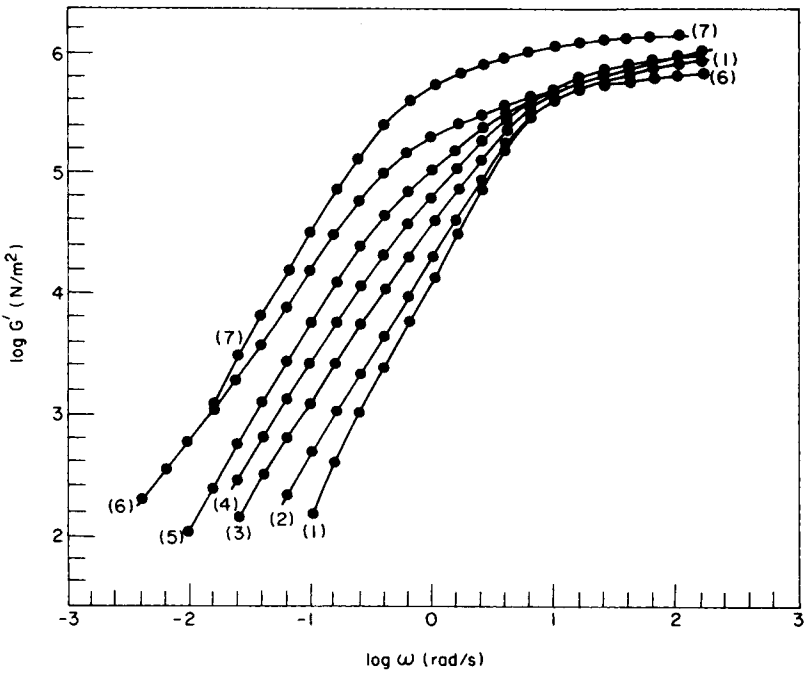

Fig. 17. Log G' vs. log ω for 174L/435L binary blends of polybutadiene at 50°C:[21] (1) 174L; (2) $\phi_2 = 0.025$; (3) $\phi_2 = 0.05$; (4) $\phi_2 = 0.1$; (5) $\phi_2 = 0.2$; (6) $\phi_2 = 0.56$; (7) 435L.

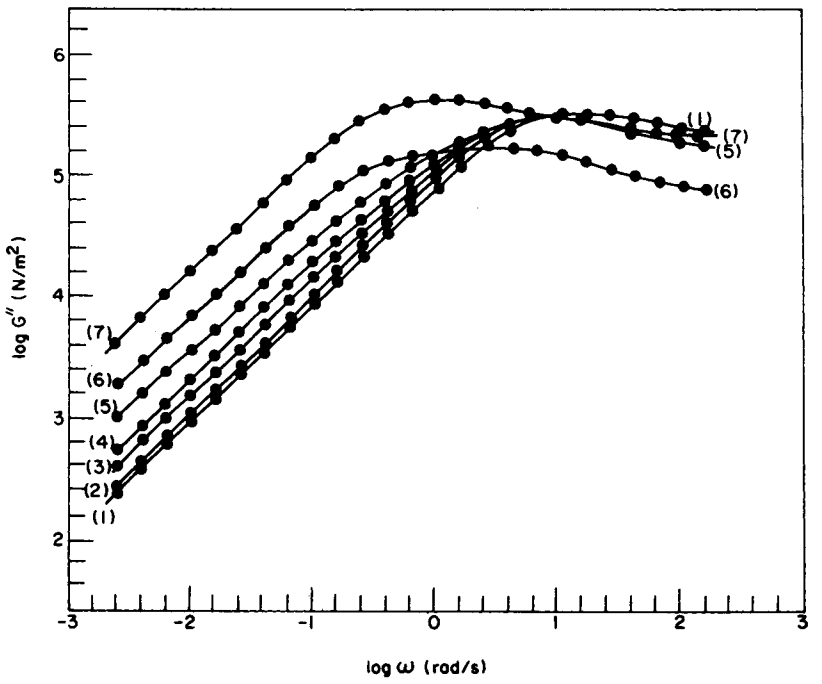

Fig. 18. Log G'' vs. log ω for 174L/435L binary blends of polybutadiene at 50°C:[21] Symbols are the same as in Fig. 17.

gated, values of G' lie between those of the constituent components. However, log G'–log G'' plots for 41L/174L binary blends, given in Figure 15, show that over the entire range of G'' investigated, values of G' at all blend compositions are larger than those of the constituent components, behavior very similar to that observed with the 41L/435L binary blends. Figure 16 shows that in the terminal region G' goes through a maximum at a certain critical blend composition and that the value of ϕ_2 at which a maximum of G' occurs depends upon G'' (i.e., the energy dissipated).

A comparison between Figures 11 and 15 indicates that the 41L/435L blends have a much greater effect of blend composition on G' than the 41L/174L blends, especially at low values of G'' (i.e., terminal region). This can be attributed to the difference in the ratio of component molecular weights, $r = M_2/M_1$. Note that r is 10.7 for the 41L/435L blends and 4.3 for the 41L/174L blends (see Table I). When r is very large in a blend of nearly monodisperse components there will be no overlap in molecular weight of the constituent components, therefore such blends may be considered to be concentrated solutions, since the low-molecular-weight component may be considered as being a homologous solvent.

Figures 17 and 18 give log G'–log ω and log G''–log ω plots, respectively, for 174L/435L binary blends at 50°C.[21] It can be seen in Figures 17 and 18 that

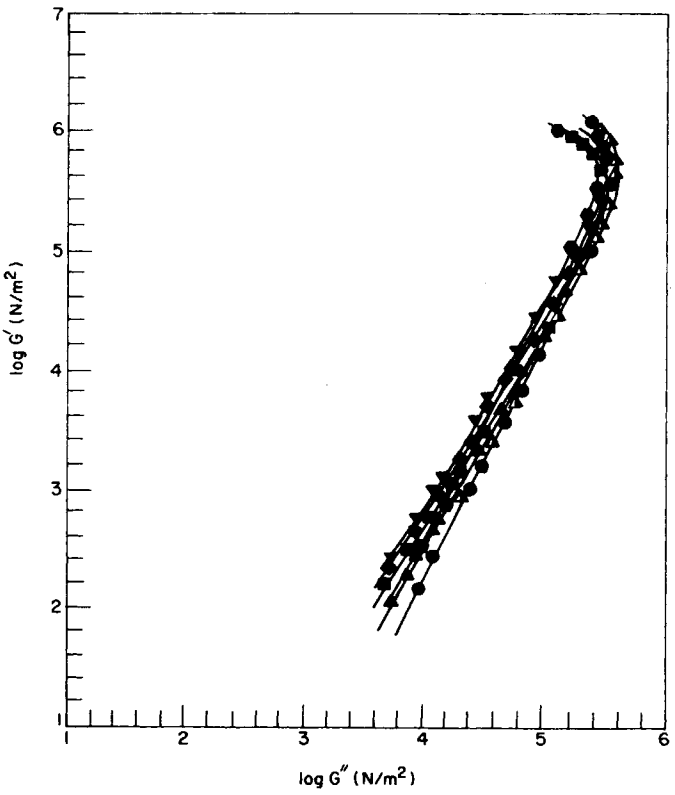

Fig. 19. Log G' vs. log G'' for 174L/435L binary blends of polybutadiene: (●) 174L; (▲) 435L; (▲) $\phi_2 = 0.025$; (■) $\phi_2 = 0.05$; (◆) $\phi_2 = 0.10$; (▼) $\phi_2 = 0.2$; (●) $\phi_2 = 0.56$.

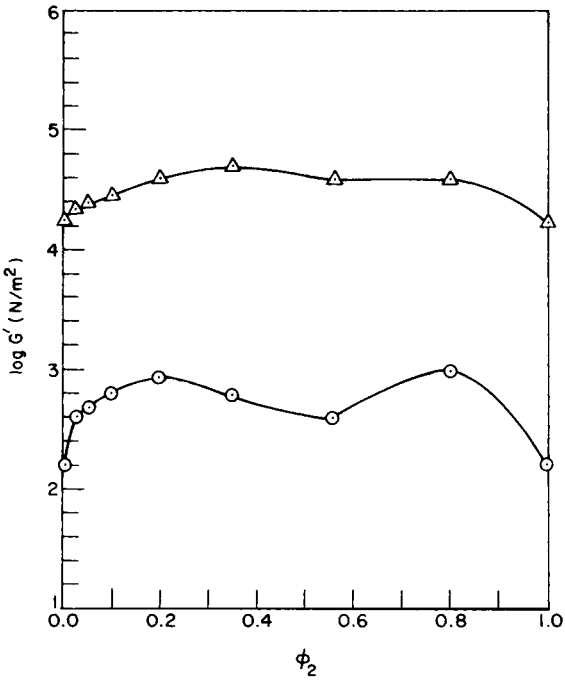

Fig. 20. Log G' vs. ϕ_2 for 174L/435L binary blends of polybutadiene at different values of G'' (N/m^2): (⊙) 10^4; (△) 10^5.

values of both G' and G'' lie between those of the constituent components in the frequency range, where G' has not reached a plateau. At high frequencies where G' already reached a plateau, some blend samples have values of G' and G'' lower than those of one of the constituent components. Such behavior was not observed with the 41L/435L and 41L/174L binary blends discussed above. Figure 19 gives $\log G'$–$\log G''$ plots for 174L/435L blends. It can be seen in Figure 19 that values of G' at all blend compositions are larger than those of the constituent components, behavior very similar to that observed with the other two blend systems discussed above, and that the dependence of G' on blend composition for the 174L/435L blend system is much more *regular* than that for the other two binary blend systems (compare Fig. 19 with Figs. 11 and 15). Note that the 174L/435L blends have a very low ratio of component molecular weights, $r = 2.5$, indicating that the difference in molecular weights between the constituent components is rather small compared to that for the other two blend systems discussed above. This small value of r for the 174L/435L binary blend system is believed to be responsible for the weak dependence of G' on blend composition observed in Figure 20.

Binary Blends of Nearly Monodisperse Polystyrenes

We will first analyze the recent experimental data of Kotaka and coworkers,[19,20] who investigated the dynamic viscoelastic properties of binary blends of nearly monodisperse polystyrenes with $M > M_e$. We will then analyze the experimental data of Montfort et al.[17] who investigated the

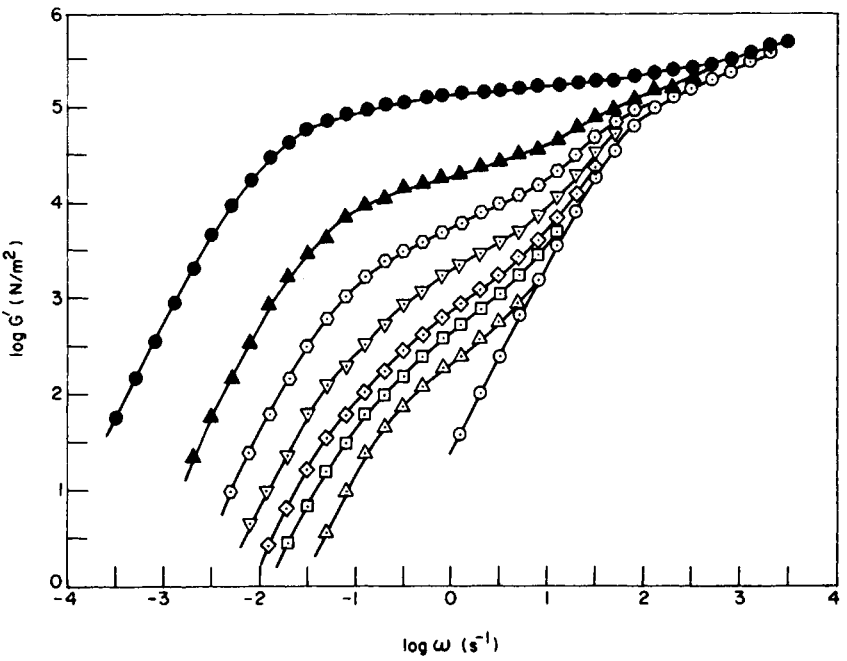

Fig. 21. Log G' vs. log ω for L427/L39 binary blends of polystyrene at 167°C:[19] (⊙) L39; (●) L427; (△) $\phi_2 = 0.01$; (⊡) $\phi_2 = 0.03$; (◇) $\phi_2 = 0.05$; (▽) $\phi_2 = 0.1$; (⊙) $\phi_2 = 0.2$; (▲) $\phi_2 = 0.4$.

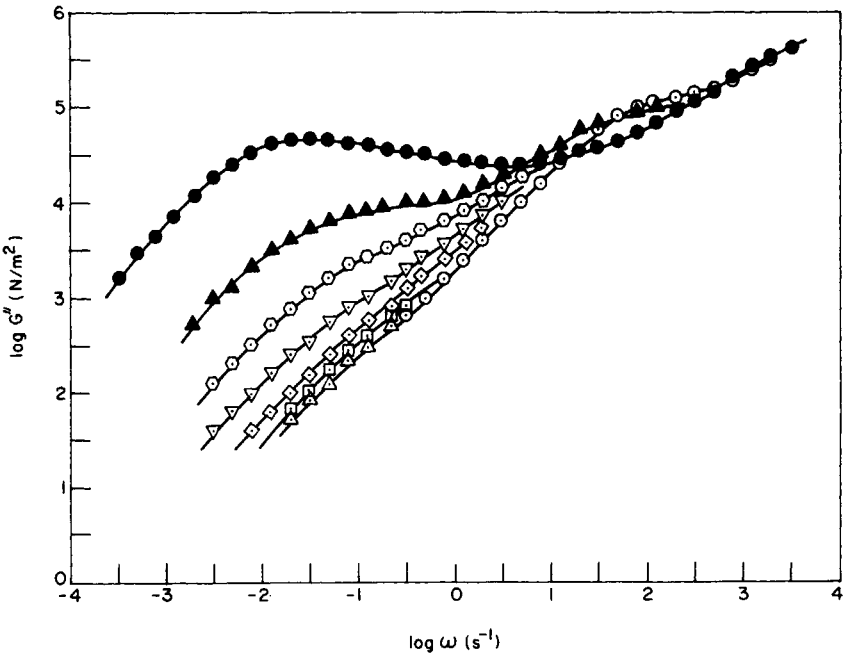

Fig. 22. Log G'' vs. log ω for L427/L39 binary blends of polystyrene at 167°C.[19] Symbols are the same as in Fig. 21.

TABLE II
Molecular Weights of the Polystyrenes Investigated by Kotaka and Co-Workers[19,20]

Sample code	$\bar{M}_w$	$\bar{M}_n$	$\bar{M}_w/\bar{M}_n$
L23	23,400	21,800	1.08
L39	38,900	36,300	1.07
L72	72,400	68,300	1.06
L89	88,500	82,700	1.07
L172	172,000	161,000	1.07
L315	315,000	294,000	1.07
L427	427,000	407,000	1.05

dynamic viscoelastic properties of binary blends of nearly monodisperse polystyrenes, one constituent component having a very high molecular weight ($M > M_c'$) and the other a very low molecular weight ($M \ll M_e$). Although there are some variations in values of M_e, M_c, and M_c' reported in the literature for polystyrene, the following values seem reasonable: M_c = 34,000 ~ 38,000, M_c/M_e = 1.8 ~ 2.1, and M_c'/M_e = 6 ~ 7.

Figures 21 and 22 give log G'–log ω and log G''–log ω plots, respectively, for L427/L39 binary blends of nearly monodisperse polystyrenes at 167°C.[19] Information on the molecular weights of the constituent components is given in Table II. Figure 23 gives log G'–log G'' plots with blend composition as a

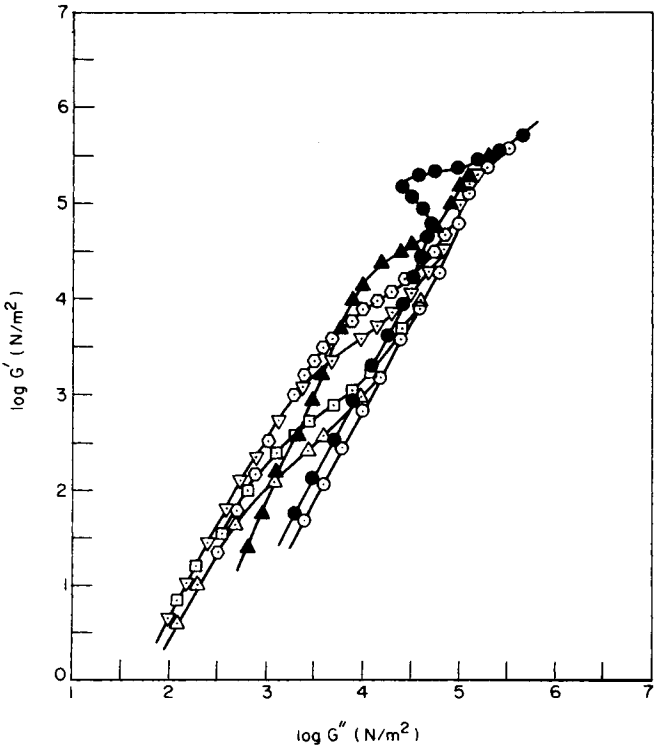

Fig. 23. Log G' vs. log G'' for L427/L39 binary blends of polystyrene. Symbols are the same as in Fig. 21.

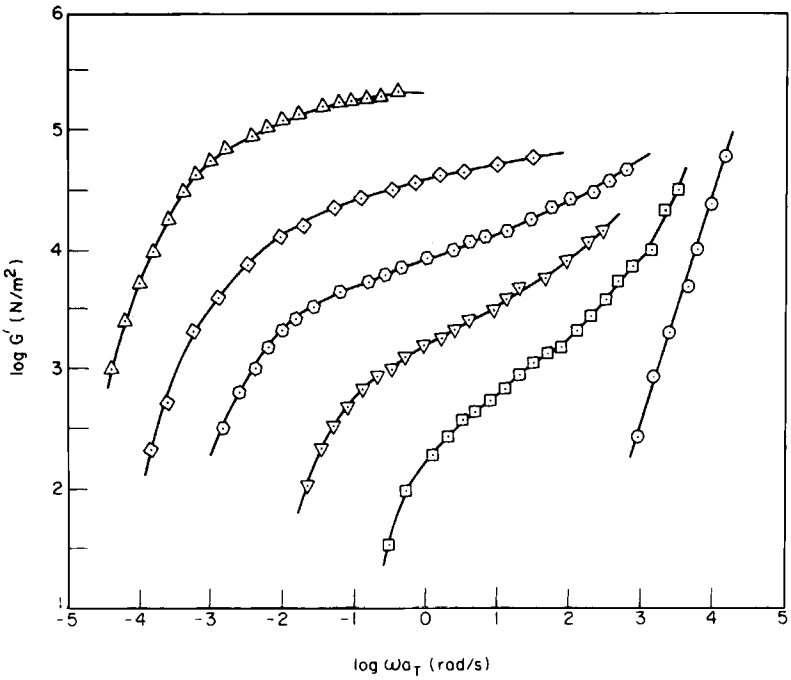

Fig. 24. Log G' vs. log ωa_T for F90/F008 binary blends of polystyrene reduced to 160°C:[36] (⊙) F008; (△) F90; (⊡) $\phi_2 = 0.05$; (▽) $\phi_2 = 0.1$; (⊙) $\phi_2 = 0.2$; (◇) $\phi_2 = 0.4$.

parameter. It can be seen in Figure 23 that despite the fact that both constituent components have molecular weights M much greater than M_e, values of G' in the terminal region for the respective constituent components do not lie on a single curve. It should be remembered that this was not the case for the nearly monodisperse polybutadienes discussed above (see Fig. 5).

Note in Figure 23 that at very small values of G'' (i.e., in the terminal region), values of G' for $\phi = 0.1$ are greater than those for $\phi = 0.01$ and also those for $\phi > 0.1$, indicating that G' goes through a maximum at $\phi = 0.1$. It can also be seen that as G'' is increased, values of G' for all blend compositions investigated approach those of the constituent component L39. The dependence of G' on blend composition in the terminal region for the L427/L39 binary blends of polystyrene is very similar to that for the 41L/174L binary blends of polybutadiene (compare Fig. 23 with Fig. 15).

Figures 24 and 25 give log G'–log ωa_T and log G''–log ωa_T plots, respectively, for F90/F008 binary blends of nearly monodisperse polystyrenes (see Table III), where a_T is a shift factor. According to Montfort,[36] the data were obtained at the following temperatures: (a) 126, 132, 139, 146, and 153°C for F008; (b) 190, 219, and 247°C for F90; (c) 125, 143, and 153°C for $\phi = 0.05$; (d) 155, 164, and 171°C for $\phi = 0.1$; (e) 158, 167, 183, and 196°C for $\phi = 0.2$; (f) 177, 187, and 197°C for $\phi = 0.4$. Since the molecular weights of F008 and F90 are 8,500 and 900,000, respectively, one can easily surmise that it would *not* have been possible to measure the dynamic viscoelastic properties of the two constituent components and their blends in the same temperature range. Therefore, we had to use frequency–temperature superposition in plotting

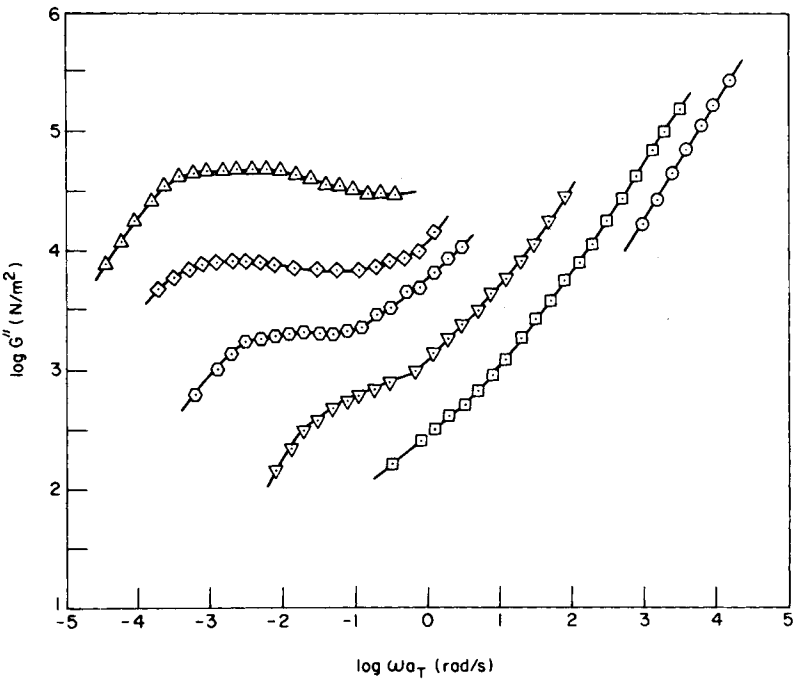

Fig. 25. Log G'' vs. log ωa_T for F90/F008 binary blends of polystyrene reduced to 160°C.[36] Symbols are the same as in Fig. 24.

TABLE III
Molecular Weights of the Polystyrenes Investigated by Montfort et al.[17]

Sample code	$\bar{M}_w$	$\bar{M}_w/\bar{M}_n$
F002	2,000	1.05
F008	8,500	1.05
F018	17,500	1.05
F11	110,000	1.05
F90	900,000	1.05

data for G' (and also data for G'') for the various blend compositions as a function of ω on a single graph.

However, in the use of $\log G'$–$\log G''$ plots, one does *not* need to use frequency-temperature superposition, as demonstrated in Figure 26 for the F90/F008 binary blends. To preserve clarity, only data at two different temperatures for each blend are displayed in Figure 26. Note that the temperature dependence is *not* noticeable, as was the case with the polybutadienes shown in Figures 6 to 8. Note further in Figure 26 that $\log G'$–$\log G''$ plots for the polystyrene F008 do not overlap those for the polystyrene F90. This is because the molecular weight (M) of F008 is 8,500, which is lower than the entanglement molecular weight (M_e), which is about 18,000. It should be remembered that according to Eq. (35), $\log G'$–$\log G''$ plots depend on M for $M < M_e$.

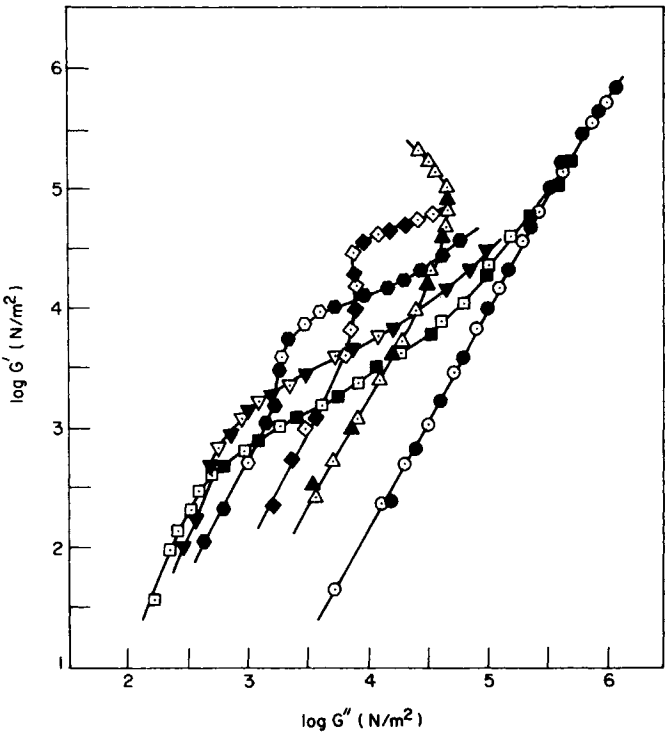

Fig. 26. Log G' vs. log G'' for F90/F008 binary blends of polystyrene: (a) F008 at 126°C (⊙) and 132°C (●); (b) F90 at 247°C (△) and 219°C (▲); (c) $\phi_2 = 0.05$ at 153°C (⊡) and 125°C (■); (d) $\phi_2 = 0.01$ at 171°C (▽) and 155°C (▼); (e) $\phi_2 = 0.2$ at 196°C (⊙) and 167°C (●); (f) $\phi_2 = 0.4$ at 177°C (◇) and 187°C (◆).

Note that the dependence of G' on blend composition for the F90/F008 binary blends of nearly monodisperse polysytrenes (shown in Fig. 26) is very similar to that for the 41L/435L binary blends of nearly monodisperse polybutadienes (shown in Fig. 11). It can be seen in Figure 26, that at very small values of G'' (i.e., in the terminal region), G' goes through a maximum at the blend composition $\phi_2 = 0.05$.

Binary Blends of Nearly Monodisperse Poly(methyl Methacrylate)s

Onogi and co-workers[7,37] have synthesized various grades of poly(methyl methacrylate)s (PMMA) by anionic polymerization and investigated the dynamic viscoelastic properties of binary blends. Table IV gives information on the molecular weights of two PMMAs, which were used in one of the binary blend systems investigated by Onogi et al.[7] Based on the ratio of weight- and number-average molecular weights, $\overline{M}_w/\overline{M}_n$ (see Table IV), the PMMAs have molecular weight distributions (MWD) slightly broader than the PBs (see Table I) and PSs (see Tables II and III) discussed above. According to Onogi and co-workers,[37] the value of M_e for PMMA varies from 6,700 to 13,100, depending on its molecular weight ($\overline{M}_w$ = 45,200–342,000). They noted that the M_c/M_e ratio for PMMA ranges from 2 to 6, though it is about 2 for the

TABLE IV
Molecular Weights of the Poly(methyl Methacrylate)s Synthesized by Onogi et al.[7]

Sample code	$\bar{M}_w$	$\bar{M}_n$	$\bar{M}_w/\bar{M}_n$
702	174,000	139,000	1.25
910	52,100	37,500	1.39

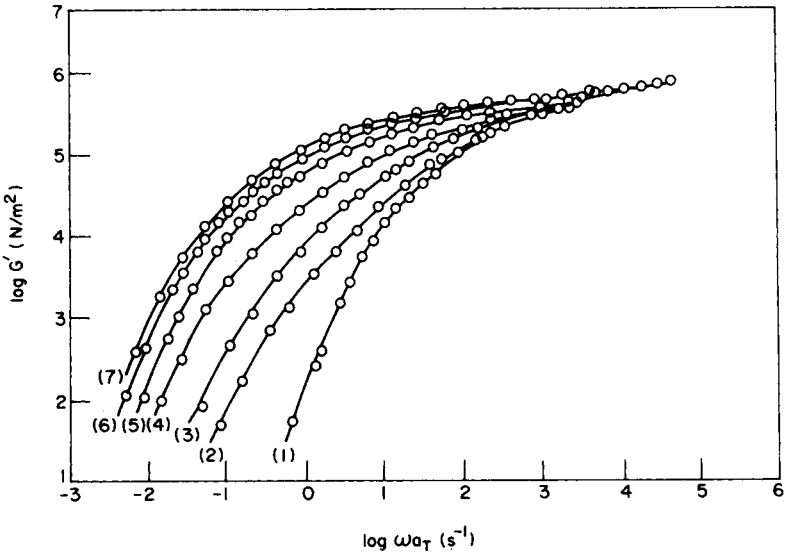

Fig. 27. Log G' vs. log ωa_T for 910/702 binary blends of poly(methyl methacrylate) reduced to 220°C as a reference temperature:[7] (1) 910, (2) $\phi_2 = 0.1$; (3) $\phi_2 = 0.23$; (4) $\phi_2 = 0.4$; (5) $\phi_2 = 0.6$; (6) $\phi_2 = 0.8$; (7) 702.

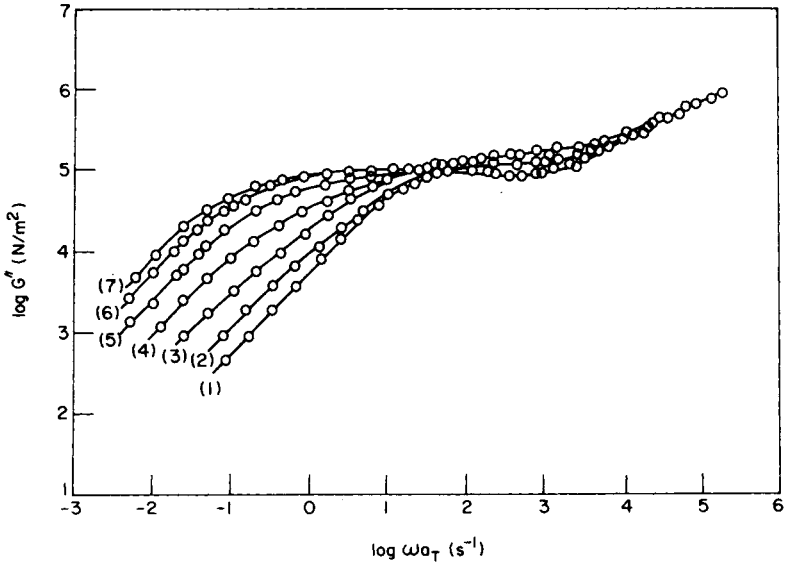

Fig. 28. Log G'' vs. log ωa_T for 910/702 binary blends of poly(methyl methacrylate) reduced to 220°C.[7] Symbols are the same as in Fig. 27.

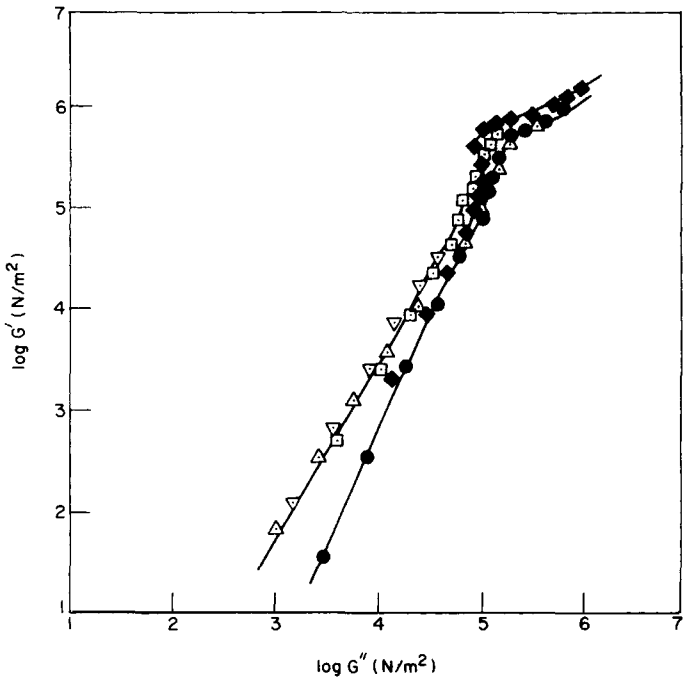

Fig. 29. Log G' vs. log G'' for 910/702 binary blends of poly(methyl methacrylate): (●) 910; (◆) 702; (△) $\phi_2 = 0.1$; (⊡) $\phi_2 = 0.4$; (▽) $\phi_2 = 0.6$.

usual nonpolar polymers. They attributed the unusally high values of M_c/M_e ratio to the polarity of PMMA, which affects its internal structure. Based on the values of M_e reported by Onogi and co-workers,[37] the molecular weights of PMMAs listed in Table IV are several times greater than the value of M_e and, therefore, they can be considered to be entangled macromolecules (i.e., $M \gg M_e$).

Figures 27 and 28 give log G'–log ωa_T and log G''–log ωa_T plots, respectively, for PMMA binary blends.[7] It can be seen in both figures that values of G' for all blends lie between those of the constituent components, whereas G'' goes through both a maximum and a minimum. However, when G' is plotted against G'' on the *logarithmic* scale (shown in Fig. 29), the dependence of G' on blend composition is not noticeable at small values of G'' (i.e., in the terminal region), which is quite different behavior from that observed above for both PB and PS binary blend systems (compare Fig. 29 with Figs. 11, 15, 19, 23, and 26). Note in Figure 29 that values of G' are insensitive to blend composition. This is attributable to the broad molecular weight distribution (MWD) of the constituent components, as judged from $\bar{M}_w/\bar{M}_n$ ratio given in Table IV.

By assuming that the MWD of the constituent components, PMMA 702 and PMMA 910, may be represented by the log-normal function $P(M)$,

$$P(M) = \frac{1}{\sigma\sqrt{2\pi}} \exp\left[-(\ln M - \ln M_o)^2/2\sigma^2\right] \tag{37}$$

where σ is the variance and M_o is a constant, we have constructed MWD curves with the aid of the values for $\bar{M}_w$ and $\bar{M}_w/\bar{M}_n$, given in Table IV. The

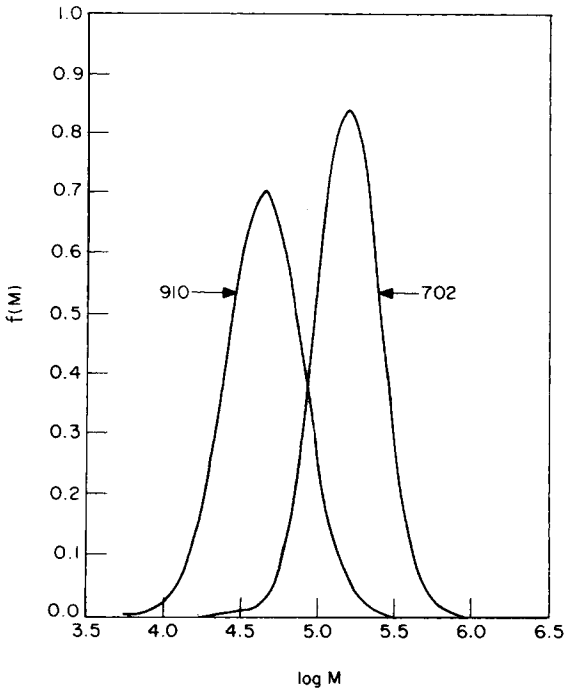

Fig. 30. Molecular weight distribution curves of the poly(methyl methacrylate)s, 910 and 702.

results are displayed in Figure 30. It can be seen in Figure 30 that there is an overlap in MWD between the PMMA 702 and PMMA 910. Note that the ratio of component molecular weights, r, for the PMMA 702 and PMMA 902 is only 3.34 (see Table IV). Therefore, it can be concluded that the overlap in MWD, observed in Figure 30, is attributable to two factors: (a) the low value of r and (b) the broad MWD of the constituent components. It is now more clear that the overlap in MWD between the constituent components is responsible for the insenstivity of $\log G'$–$\log G''$ plots to blend composition, observed in Figure 29.

ANALYSIS OF THE LINEAR VISCOELASTIC PROPERTIES OF BINARY BLENDS OF COMMERCIAL POLYMERS

We will now discuss linear viscoelastic properties of binary blends of commercial polymers, that were determined in our laboratory. The polymers investigated together with their molecular weights are listed in Table V. Here it can be seen that all of the polymers used have broad MWDs. Various binary blend compositions were prepared using a twin-screw compounding machine and their dynamic viscoelastic properties were determined using a Model 16 Weissenberg Rheogoniometer at various temperatures.

Binary Blends of Low-Density Polyethylenes

Figure 31 gives $\log G'$–$\log \omega$ and $\log G''$–$\log \omega$ plots for binary blends of commercial low-density polyethylenes (LDPE) (U.S. Industrial Chemical Company) at 180°C. It can be seen that values of G' and G'' for all blends lie

TABLE V
Molecular Weights of the Commercial Polymers Investigated

Sample code	$\bar{M}_w$	$\bar{M}_n$	$\bar{M}_w/\bar{M}_n$
	(a) LDPE blends		
MN714	176,000	14,400	7.5
MN722	103,000	17,600	5.9
	(b) PMMA/PVDF blends		
PMMA	77,100	18,500	4.1
PVDF	180,000	60,000	3.0
	(c) SAN/PCL blends		
SAN	150,000	72,000	2.1
PCL	40,000	15,000	2.7
	(d) SAN/PMMA blends		
SAN	150,000	72,000	2.1
PMMA	77,100	18,500	4.1

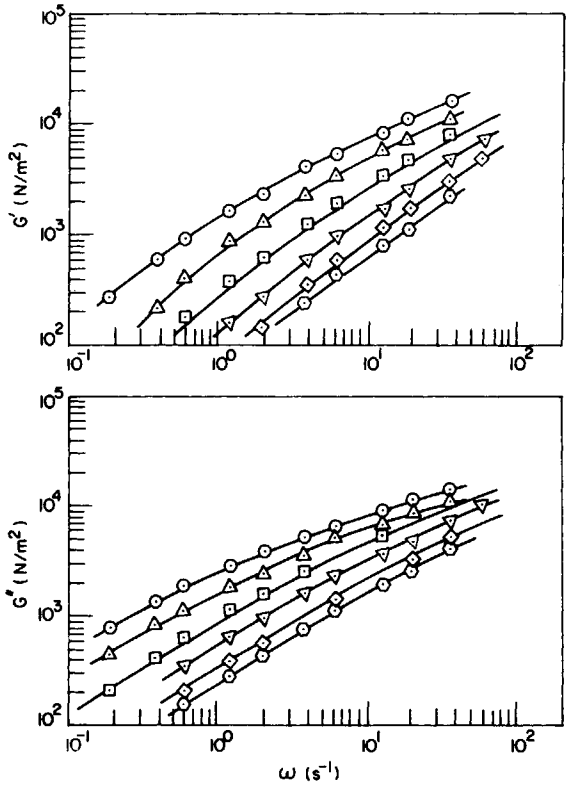

Fig. 31. Log G' vs. log ω, and log G'' vs. log ω, for MN722/MN714 binary blends of low-density polyethylene at 180°C;[25] (⊙) MN722; (⊙) MN714; (◇) $\phi_2 = 0.2$; (▽) $\phi_2 = 0.4$; (⊡) $\phi_2 = 0.6$; (△) $\phi_2 = 0.8$.

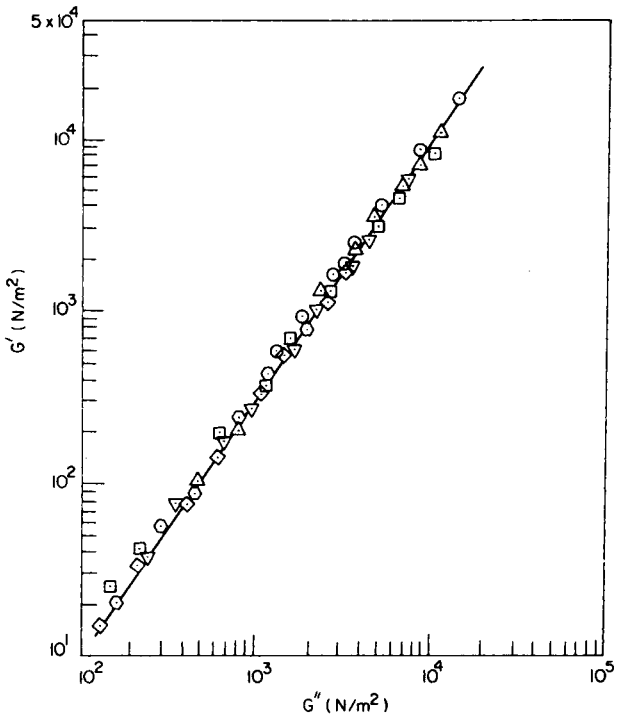

Fig. 32. Log G' vs. log G'' for MN722/MN714 binary blends of low-density polyethylene. Symbols are the same as in Fig. 31.

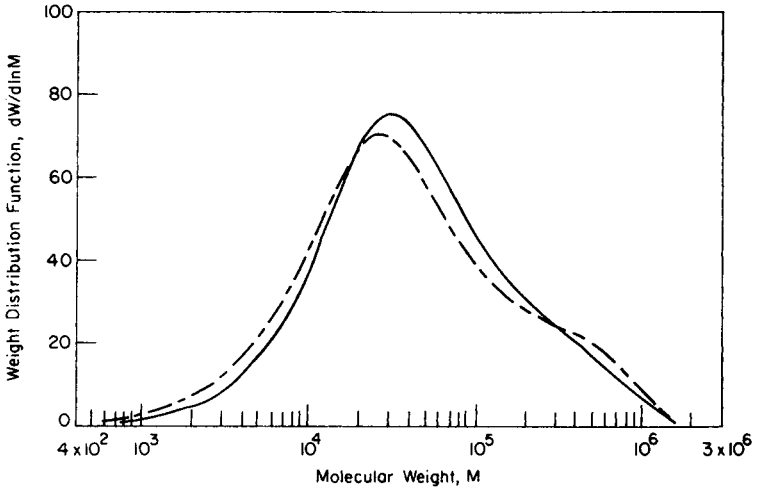

Fig. 33. Molecular weight distribution curves of low-density polyethylenes: (——) MN722; (---) MN714.

between those of the constituent components. However, when G' is plotted against G'' on the logarithmic scale (Fig. 32) we observe that all blends and constituent polymers lie on a single curve. This somewhat surprising observation can be explained from the conclusion drawn above with respect to the PMMA binary blends (see Fig. 29), that is, it stems from the fact that the constituent polymers have very broad MWDs that overlap substantially (Fig. 33).

Binary Blends of Compatible Polymers Having Dissimilar Chemical Structures

We will now discuss the linear viscoelastic properties of binary blends of compatible polymers having dissimilar chemical structures, namely, (a) binary blends of poly(methyl methacrylate) (PMMA) and poly(vinylidene fluoride) (PVDF), (b) binary blends of poly(methyl methacrylate) (PMMA) and poly(styrene-*co*-acrylonitrile) (SAN), and (c) binary blends of poly(ϵ-caprolactone) (PCL) and ploy(styrene-*co*-acrylonitrile) (SAN).

Figure 34 gives $\log G'$–$\log \omega$ and $\log G''$–$\log \omega$ plots for binary blends of PMMA (Plexiglas 750, Rohm and Haas Co.) and PVDF (Kynar 960, Pennwalt

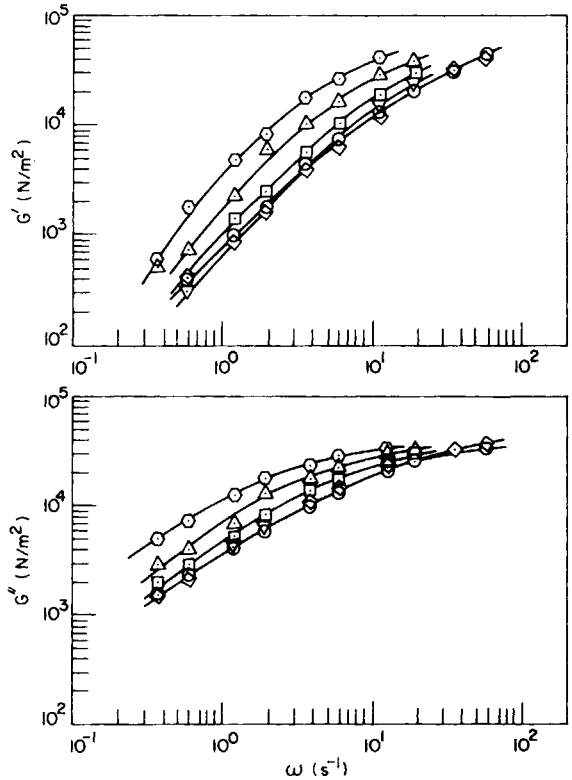

Fig. 34. Log G' vs. log ω, and log G'' vs. log ω, for binary blends of poly(methyl methacrylate) (PMMA) and poly(vinylidene fluoride) (PVDF) at 210°C 210°C;[25]: (○) PMMA; (⊙) PVDF; (◇) PMMA/PVDF = 20/80; (▽) PMMA/PVDF = 40/60; (□) PMMA/PVDF = 60/40; (△) PMMA/PVDF = 80/20.

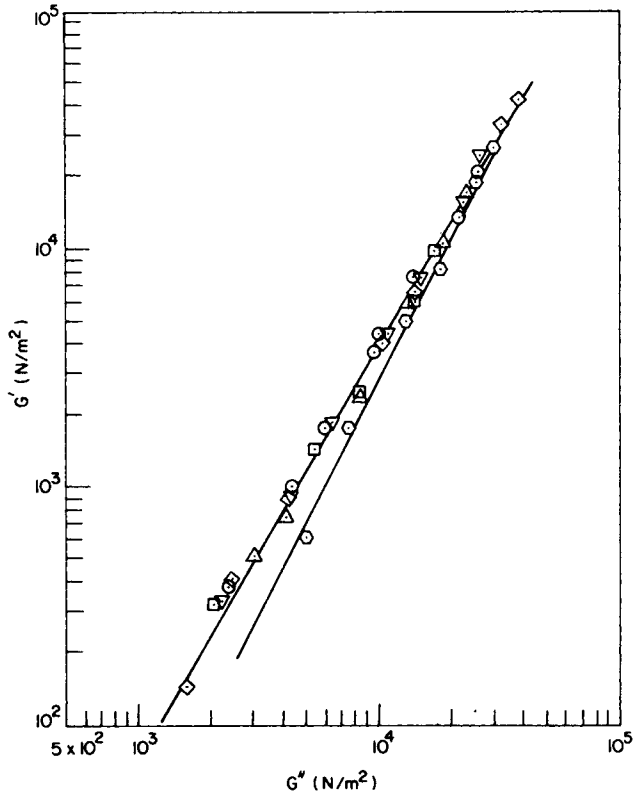

Fig. 35. Log G' vs. log G'' for binary blends of poly(methyl methacrylate) and poly(vinylidene fluoride) at 210°C. Symbols are the same as in Fig. 34.

Corporation) at 210°C. A number of investigators[38-41] have reported that blends of PMMA and PVDF are compatible on a molecular level. Information on the molecular weights of the PMMA and PVDF investigated is given in Table V. Figure 35 gives log G'–log G'' plots for the PMMA/PVDF blends. It can be seen in Figure 35 that data points for all blend samples lie between those of the constituent polymers, showing a strong trend where most of the blends' data lie very close to the upper curve, representing the PVDF. The fact that few data points of the blends have values of G' greater than those of the PVDF (i.e., the upper curve) is attributable to the broad MWD of the constituent polymers. Note in Figure 35 that the constituent polymers have different values of G', especially in the terminal region, which implies that the PVDF is more elastic than the PMMA. This is very reasonable, since the elasticity of polymers varies with molecular structure. And it would be quite unlikely to observe the same fluid elasticity for two dissimilar polymers.

Figure 36 gives log G'–log G'' plots for binary blends of PMMA (Plexiglas 750) (Rohm and Haas Co.) and SAN (Tyril 1000, Dow Chemical Co.) at 220°C. The two curves drawn through the data points represent the respective constituent polymers. For the sake of clarity, the data obtained at other temperatures are not shown in Figure 36. Information on the molecular

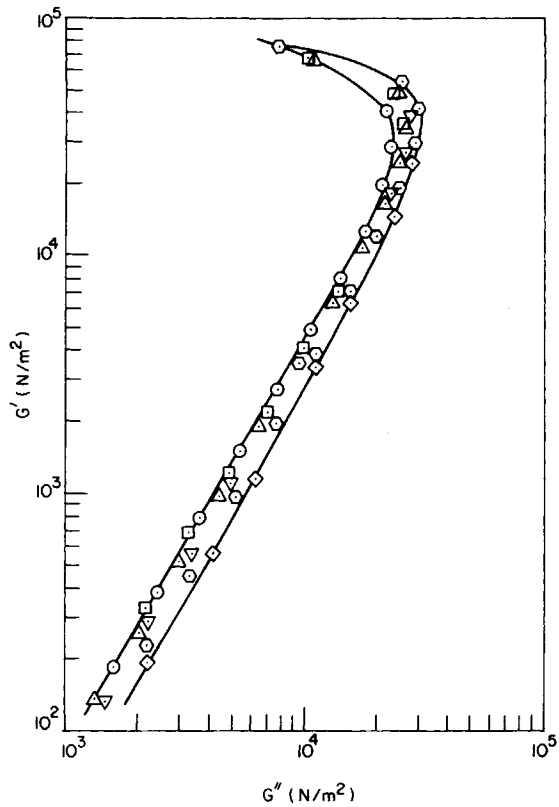

Fig. 36. Log G' vs. log G'' for binary blends of poly(styrene-*co*-acrylonitrile) (SAN) and poly(methyl methacrylate) (PMMA) at 220°C:[26] (⊙) SAN; (◇) PMMA; (△) SAN/PMMA = 80/20; (⊡) SAN/PMMA = 60/40; (▽) SAN/PMMA = 40/60; (⊙) SAN/PMMA = 20/80.

weights of the PMMA and SAN is given in Table V. A number of investigators[42-47] have reported that blends of PMMA and SAN are compatible.

It can be seen (Fig. 36) that the SAN is more elastic than the PMMA and that values of G' for the binary blends lie between those of the constituent polymers. Similar to the situation observed with the PMMA/PVDF binary blends (Fig. 35), in Figure 36 there is a strong trend for the values of G' of most of the blend samples to lie close to the upper curve, representing the SAN. Again, it is believed that this is due to the broad MWD of the constituent polymers (see Table V).

Figure 37 gives log G'–log G'' plots for binary blends of PCL (PCL-700, Union Carbide Co.) and SAN (Tyril 1000, Dow Chemical Co.). Information on the molecular weights of the PCL and SAN investigated is given in Table V. Blends of PCL and SAN are known to be compatible (48–51). The PCL had the melting point of about 60°C with thermal degradation of PCL occurring at temperatures above 160°C. Therefore, rheological measurements for the PCL were made at temperatures below 160°C. On the other hand, rheological measurements for the SAN were made at temperatures above 200°C, since the SAN was very viscous at temperatures below 200°C. Consequently, the rheological measurements of the PCL/SAN binary blends were made at

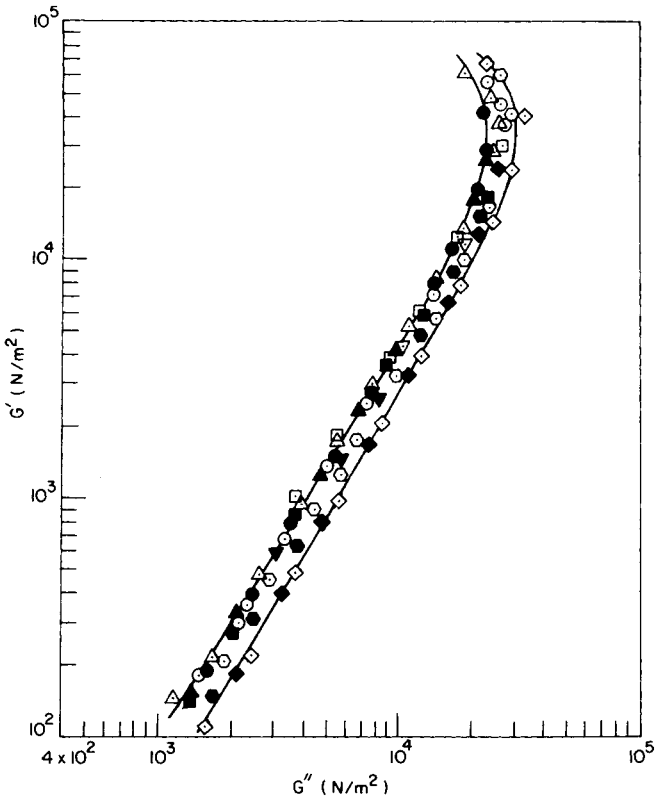

Fig. 37. Log G' vs. log G'' for binary blends of poly(ϵ-caprolactone) (PCL) and poly(styrene-*co*-acrylonitrile) (SAN):[26] (a) SAN at 200°C (⊙) and 220°C (●); (b) PCL at 100°C (◇) and 120°C (◆); (c) SAN/PCL = 80/20 at 180°C (△) and 200°C (▲); (d) SAN/PCL = 60/40 at 140°C (⊡) and 160°C (■); (e) SAN/PCL = 40/60 at 140°C (▽) and 160°C (▼); (f) SAN/PCL = 20/80 at 120°C (⊙) and 140°C (●).

temperatures between 120°C and 200°C, depending upon the blend compositions employed. Nevertheless, the use of log G'–log G'' plots enabled the correlation of linear viscoelastic properties of the PCL/SAN binary blends, without having to rely on frequency-temperature superposition.

It can be seen in Figure 37 that values of G' for all blend samples lie between those of the constituent polymers, and that most of the data points for blend samples tend to lie close to the upper curve, representing the SAN. This behavior is very much the same as that observed above for the PMMA/PVDF and PMMA/SAN binary blends.

PREDICTION OF THE LINEAR VISCOELASTIC PROPERTIES OF BINARY BLENDS

In order to predict the experimental results presented above for binary blends of nearly monodisperse polymers, a blending law proposed by Montfort et al.[14] was used. Briefly stated, they have proposed that Eq. (15) be extended

to predict the complex viscosity of a binary blend, $\eta_b^*(\omega)$

$$[\eta_b^*(\omega)]^{1/p} = (1 - \alpha)[\eta_1^*(\omega)]^{1/p} + \alpha[\eta_2^*(\omega)]^{1/p} \tag{38}$$

where $\eta_1^*(\omega)$ and $\eta_2^*(\omega)$ are complex viscosities of the components 1 and 2, respectively, p is an adjustable parameter, and α is given by

$$\alpha = \frac{(1 - \phi_2 + r\phi_2)^{3.4/p} - 1}{r^{3.4/p} - 1} \tag{39}$$

where r is the ratio of component molecular weights, M_2/M_1. Note that for $p = 3.4$ and as $\omega \to 0$, Eq. (38) reduces to Eq. (15). Since the complex modulus $G^*(\omega)$ is related to the complex viscosity $\eta^*(\omega)$ by $G^*(\omega) = i\omega\eta^*(\omega)$, Montfort et al.[14] have proposed that Eq. (38) be extended to predict the complex modulus of a binary blend, $G_b^*(\omega)$

$$[G_b^*(\omega)]^{1/p} = (1 - \alpha)[G_1^*(\omega)]^{1/p} + \alpha[G_2^*(\omega)]^{1/p} \tag{40}$$

where $G_1^*(\omega)$ and $G_2^*(\omega)$ are the complex moduli of the constituent components 1 and 2, respectively, and α is given by Eq. (39).

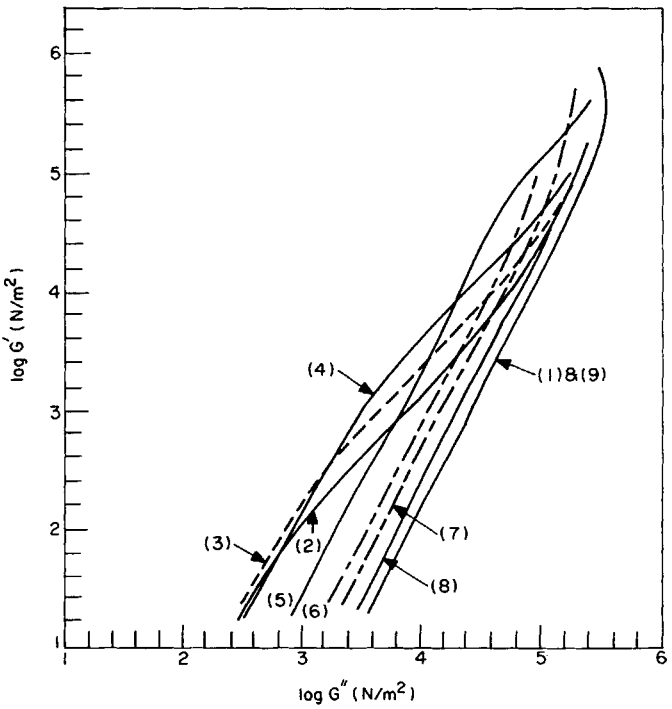

Fig. 38. Theoretically predicted $\log G'$–$\log G''$ plots for 41L/435L binary blends of polybutadiene: (1) 41L; (2) $\phi_2 = 0.025$; (3) $\phi_2 = 0.05$; (4) $\phi_2 = 0.10$; (5) $\phi_2 = 0.36$ (6) $\phi_2 = 0.5$; (7) $\phi_2 = 0.7$; (8) $\phi_2 = 0.9$; (9) 435L.

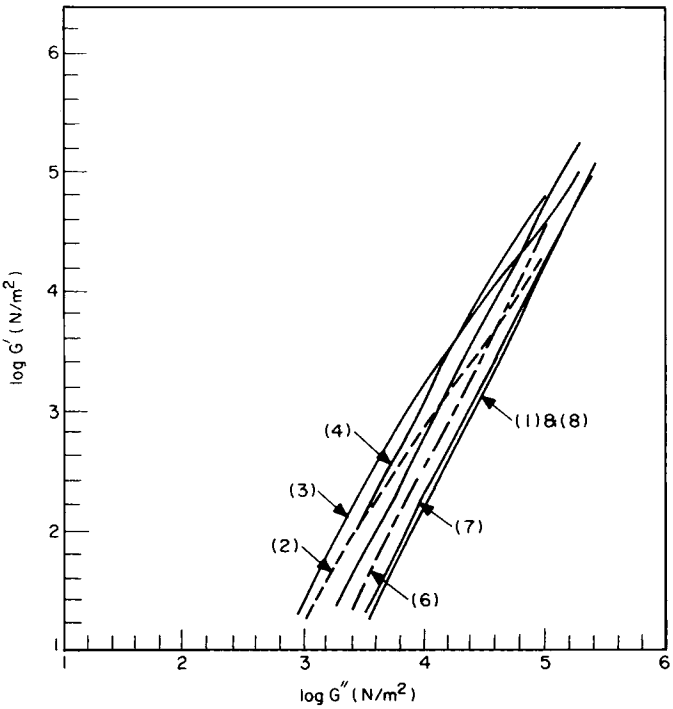

Fig. 39. Theoretically predicted $\log G'$–$\log G''$ plots for 41L/174L binary blends of polybutadiene: (1) 41L; (2) $\phi_2 = 0.025$; (3) $\phi_2 = 0.1$; (4) $\phi_2 = 0.3$; (5) $\phi_2 = 0.5$; (6) $\phi_2 = 0.7$; (7) $\phi_2 = 0.9$; (8) 174L.

In the present study, with the experimental data for $G'(\omega)$ and $G''(\omega)$ for the constituent components, 41L, 174L, and 435L (see Figs. 3 and 4), we have computed first $G_1^*(\omega)$ and $G_2^*(\omega)$ and then $G_b^*(\omega)$ with the aid of Eq. (40), and finally the real and imaginary parts, $G_b'(\omega)$ and $G_b''(\omega)$, in order to construct $\log G'$–$\log G''$ plots for the three sets of binary blends (41L/435L, 41L/174L, and 174L/435L blends) of nearly monodisperse polybutadienes. The computed results are plotted in Figures 38 to 40. It can be seen in these figures that the predicted dependence of G' on blend composition in $\log G'$–$\log G''$ plots agrees remarkably well with the experimental results given in Figures 11, 15, and 19. It should be mentioned that in constructing Figures 38 to 40, we had to extrapolate the data of Struglinski[21] to the low-frequency range, following the procedure described by Montfort et al.[14] In the theoretical predictions presented in Figures 38 to 40, the value of p was set equal to 10 and then the average relaxation time, τ_o, was calculated with the relationship $\tau_o = \eta_o J_e^o$, using the following numerical values:[22] (a) For 41L at 25°C, $\eta_o = 1.35 \times 10^3$ N.s/m^2 and $J_e^o = 1.8 \times 10^{-6}$ m^2/N; (b) For 174L at 25°C, $\eta_o = 2.95 \times 10^5$ N.s/m^2 and $J_e^o = 9.33 \times 10^{-7}$ m^2/N; (c) For 435L at 25°C, $\eta_o = 4.80 \times 10^6$ N.s/m^2 and $J_e^o = 1.8 \times 10^{-7}$ m^2/N.

In presenting the linear viscoelastic properties of binary blends of homopolymers having broad MWDs, we have adopted the procedure suggested by Montfort et al.[15] Briefly stated, the procedure calls for computation of the complex modulus of a polydisperse polymer $G^*(\omega)$ with the following expres-

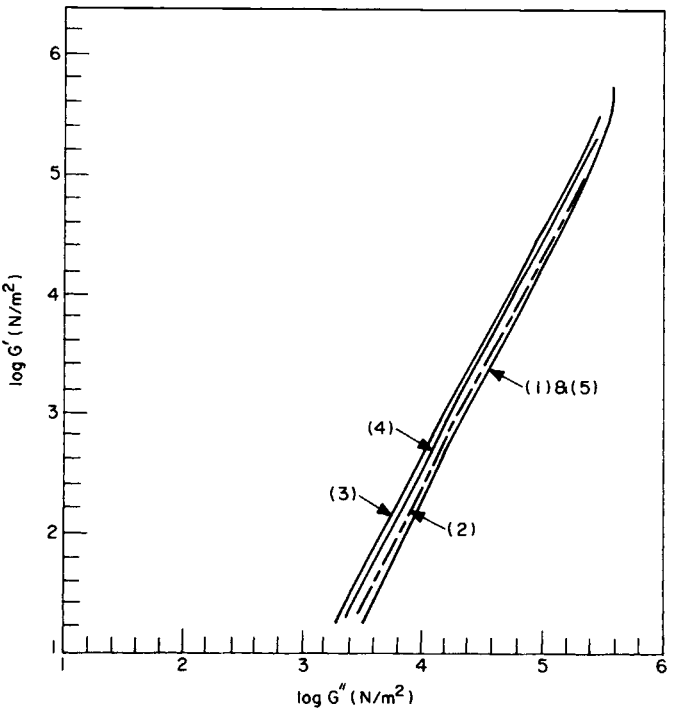

Fig. 40. Theoretically predicted log G'–log G'' plots for 174L/435L binary blends of polybutadiene: (1) 174L; (2) $\phi_2 = 0.025$; (3) $\phi_2 = 0.2$; (4) $\phi_2 = 0.56$; (5) 435L.

sion:

$$G^*(\omega) = \left\{ \int_{-\infty}^{\infty} [G_M^*(\omega)]^{1/3.4} f(M)\, d \ln M \right\}^{3.4} \tag{41}$$

where $G_M^*(\omega)$ is the complex modulus of a fraction with molecular weight M and $f(M)$ is the weight-fraction differential molecular weight distribution function defined as

$$f(M) = dW(M)/d \ln M \tag{42}$$

Note that $dW(M)$ in Eq. (42) represents the weight fraction of the sample whose molecular weights lie between $\ln M$ and $(\ln M + d \ln M)$. To use Eq. (41) for computing $G^*(\omega)$, one must have information about the dependence of $G_M^*(\omega)$ on molecular weight M and functional representation of $f(M)$ for the constituent components. According to Montfort et al.,[15] $G_M^*(\omega)$ may be related to molecular weight M of a monodisperse polymer by the expression:

$$[G_M^*(\omega)]^{-1} = \frac{1}{i\omega\eta_o} + \frac{J_p}{1 + (i\omega\tau_p)^{1-\alpha}} + \frac{J_t}{1 + (i\omega\tau_t)^{1-\beta}} \tag{43}$$

Using anionically polymerized polystyrenes, Montfort et al.[15] have found that η_o and τ_p in Eq. (43) are dependent upon molecular weight M, that is

TABLE VI
Summary of the Parameters in the Log-Normal Distribution Function for Polydisperse Polystyrenes

Sample code	$\bar{M}_w$	$\bar{M}_w/\bar{M}_n$	M_o	σ
PS1	4.03×10^5	3.1	2.29×10^5	1.0647
PS2	1.06×10^6	3.1	6.00×10^5	1.0647
PS3	3.17×10^6	3.1	1.80×10^6	1.0647
PS4	2.19×10^6	13.3	6.00×10^5	1.6094

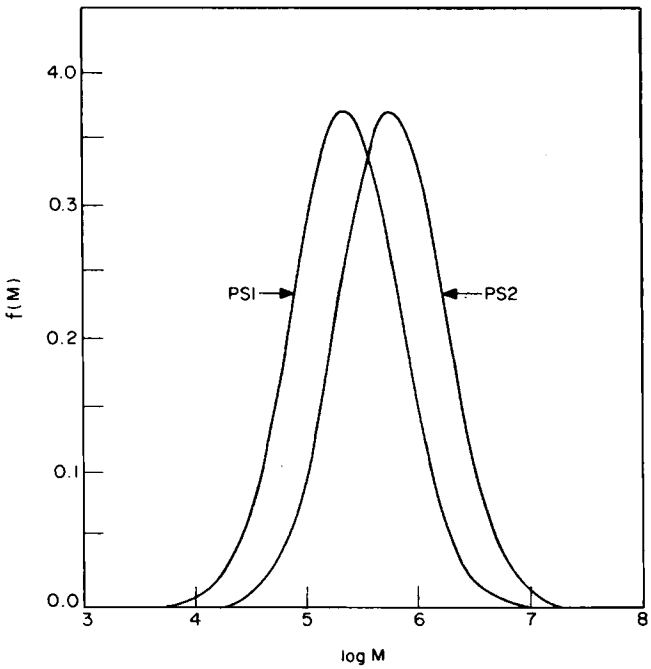

Fig. 41. Molecular weight distribution curves for polystyrenes, PS1 and PS2.

$\eta_o = 3.98 \times 10^{-13} M^{3.4}$ N.s/m^2 and $\tau_p = 2.24 \times 10^{-19} M^{3.31}$ s, and have given the following numerical values for other parameters appearing in Eq. (43): $J_p = 4.5 \times 10^{-6}$ m^2/N; $J_t = 7.5 \times 10^{-6}$ m^2/N; $\tau_t = 2 \times 10^{-3}$ s; $\alpha = 0.3$; $\beta = 0.3$. For demonstration purposes, we have used the numerical values given above for polystyrene and the molecular weight distribution function defined by Eq. (37). Table VI gives a summary of the weight-average molecular weight $\bar{M}_w$, polydispersity $\bar{M}_w/\bar{M}_n$ and the parameters σ and M_o for the four polydisperse polystyrenes considered. Specifically, we have considered the following three binary blend systems, namely, PS1/PS2, PS1/PS3, and PS1/PS4. Figures 41 to 43 give MWD curves for the PS1/PS2, PS1/PS3, and PS1/PS4 blends, respectively.

In the present investigation, we have computed the dynamic storage and loss moduli, $G_b'(\omega)$ and $G_b''(\omega)$, of a binary blend of polydisperse polystyrenes according to the following steps: (1) values of $G_M'(\omega)$ and $G_M''(\omega)$ were computed for various values of molecular weight, using Eq. (43) and then

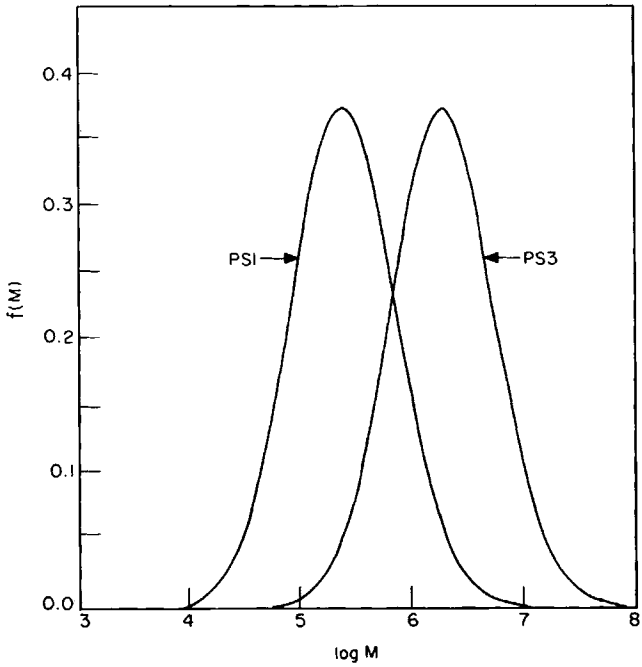

Fig. 42. Molecular weight distribution curves for polystyrenes, PS1 and PS3.

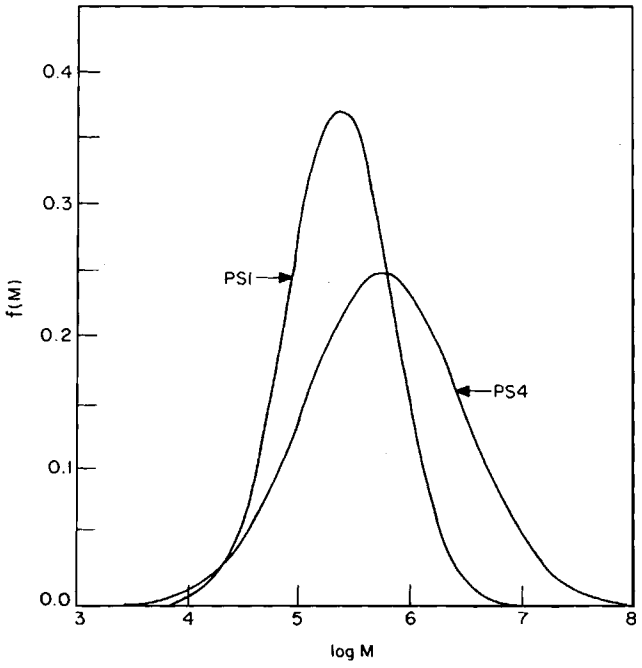

Fig. 43. Molecular weight distribution curves for polystyrenes, PS1 and PS4.

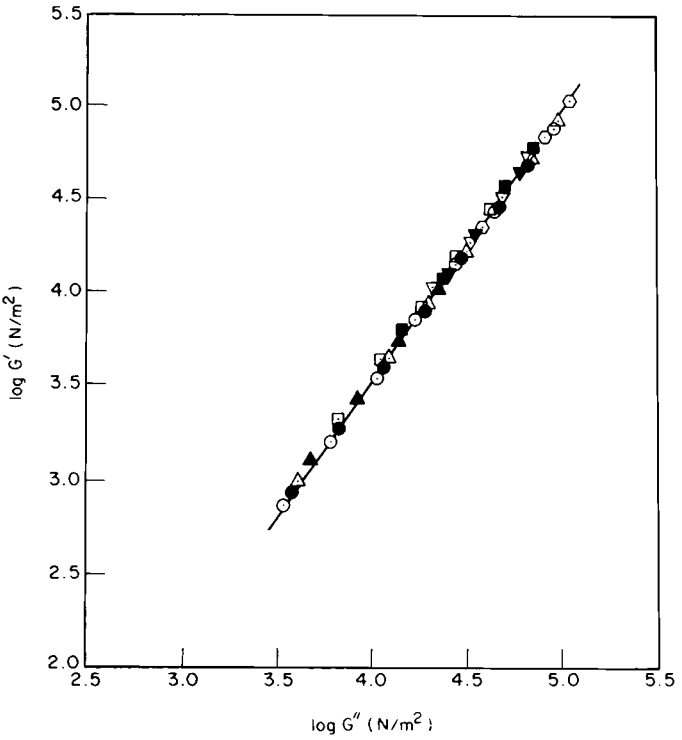

Fig. 44. Theoretically predicted $\log G'$–$\log G''$ plots for PS1/PS2 binary blends: (⊙) PS1; (⊙) PS2; (●) $\phi_2 = 0.025$; (△) $\phi_2 = 0.05$; (▲) $\phi_2 = 0.1$; (⊡) $\phi_2 = 0.2$; (■) $\phi_2 = 0.5$; (▽) $\phi_2 = 0.7$; (▼) $\phi_2 = 0.9$.

values of $[G_M^*(\omega)]^{1/3.4}$; (2) the real and imaginary parts, respectively, of $[G_M^*(\omega)]^{1/3.4}$ were integrated numerically, using Eq. (41), from $-\infty$ to $+\infty$ to obtain values of $G_i^*(\omega)$ $(i = 1, 2)$ for the constituent components with the aid of Eq. (37); and (3) values of $G_b^*(\omega)$ for a binary blend were computed with the aid of Eq. (40) and then the real and imaginary parts, $G_b'(\omega)$ and $G_b''(\omega)$ respectively, of $G_b^*(\omega)$ were computed.

Figure 44 gives computed results of $\log G'$–$\log G''$ plots for the PS1/PS2 binary blends at various blend compositions. Similar results are given in Figure 45 for the PS1/PS3 binary blends and in Figure 46 for the PS1/PS4 binary blends. It is of interest to note in Figure 44, that hardly any effect of blend composition is observed in the $\log G'$–$\log G''$ plots for the PS1/PS2 binary blend system. This can be attributed to: (1) the nature of the MWD curves of the constituent components, PS1 and PS2, which have considerable overlap (see Fig. 41) and (2) a relatively small difference in average molecular weight between the constituent components. Note in Table VI that the ratio of the component weight-average molecular weights is 2.63 for the PS1/PS2 blends. This can also explain why the $\log G'$–$\log G''$ plots of binary blends of commercial low-density polyethylenes, given in Figure 32, show little sensitivity to blend composition (see Fig. 33 for the MWD curves for the two LDPEs).

However, when the MWD curves of the constituent components overlap less and the ratio of component molecular weights is increased from 2.63

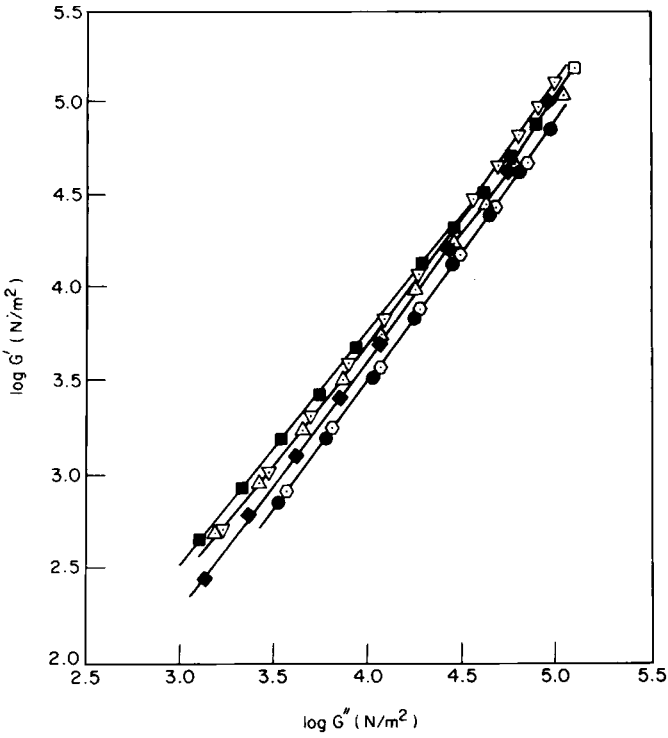

Fig. 45. Theoretically predicted log G'–log G'' plots for PS1/PS3 binary blends: (●) PS1; (⊙) PS3; (△) $\phi_2 = 0.1$; (■) $\phi_2 = 0.2$; (▽) $\phi_2 = 0.5$; (◆) $\phi_2 = 0.7$.

to 7.84, the effect of blend composition on G' becomes noticeable in the log G'–log G'' plots, as may be seen in Figure 45. Note in Figure 45 that the constituent components have the same values of G' and that the values of G' for the binary blends are greater than those of the constituent components, that is G' goes through a maximum at a certain critical blend composition. It should be noted that the constituent components, PS1 and PS3, have the same degree of polydispersity, but different molecular weights. In such a case, the MWD curve of the high-molecular-weight component is shifted along the axis of molecular weight, while maintaining the same shape (compare Fig. 42 with Fig. 41).

On the other hand, when the constituent components have differently shaped MWD curves (see Fig. 43), values of G' for a constituent component with broader MWD and higher average molecular weight, are greater than those of the other constituent component with narrower MWD and lower average molecular weight. The theoretical predictions of log G'–log G'' plots for the PS1/PS4 binary blends are given in Figure 46. It is of interest to note in Figure 46, that values of G' for the binary blends are confined between those of the constituent components; however, there is a strong trend for values of G' of the blends with $\phi > 0.2$ to lie on the upper line, which represents the PS4. This behavior is exactly the same as was observed with the binary blends of commercial polymers considered above, namely, PVDF/PMMA, PCL/SAN, and PMMA/SAN blend systems (see Figs. 35 to

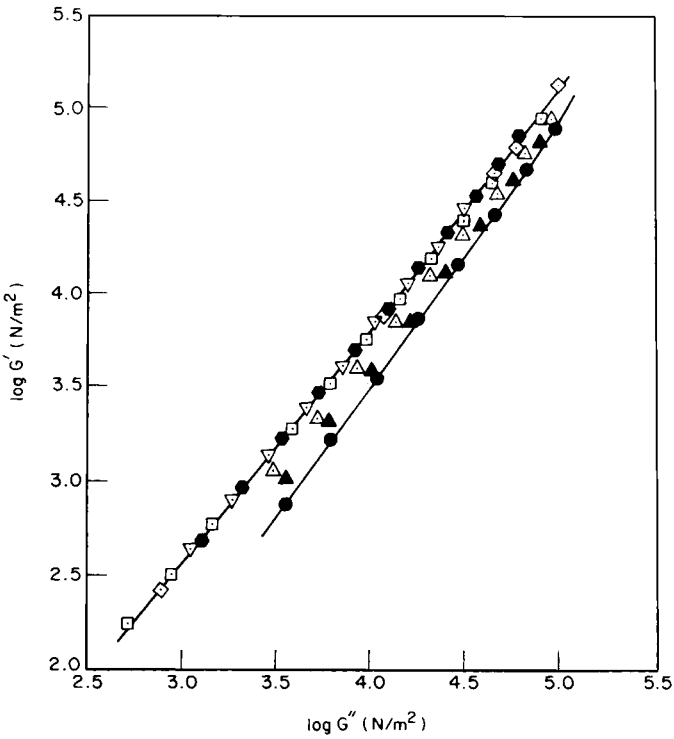

Fig. 46. Theoretically predicted log G'–log G'' plots for PS1/PS4 binary blends: (●) PS1; (●) PS4; (▲) $\phi_2 = 0.1$; (△) $\phi_2 = 0.2$; (⊡) $\phi_2 = 0.4$; (▽) $\phi_2 = 0.6$; (◇) $\phi_2 = 0.8$.

37). Considering that the commercial polymers, PMMA, PVDF, SAN, and PCL all have broad MWDs and different polydispersity (see Table V), we can now conclude that the observed dependence of G' on blend composition in log G'–log G'' plots, given in Figures 35 to 37, for the binary blends of these commercial polymers is due to the existence of a substantial overlap in molecular weight between the constituent components and to different degrees of polydispersity of the respective constituent components.

CONCLUDING REMARKS

It has been reported in the literature[3-5,8,12-18,21-23] that when the ratio of component molecular weights is greater than 1, plots of J_{eb}^o versus ϕ_2 for a binary blend system consisting of nearly monodisperse constituent components show a maximum at a certain critical blend composition (see Fig. 1). It should be noted from Eq. (2) that plots of J_{eb}^o versus ϕ_2 are obtained in the limit as the angular frequency ω approaches zero (i.e., $\omega \to 0$), therefore such plots cannot provide information on how the rate of deformation influences the fluid elasticity of binary blends. However, once plots of log G' versus log G'' are constructed with blend composition ϕ_2 as a parameter, one can easily prepare plots of G' versus ϕ_2 with G'' as a parameter. Note that the plots of G' versus ϕ_2 with G'' as a parameter show a maximum at a certain critical blend composition when the ratio of component molecular weights is

greater than 1 (see Figs. 12 and 16). Since G'' represents the energy dissipated during flow, plots of G' versus ϕ_2 with G'' as a parameter may be used for describing how the rate of deformation influences the fluid elasticity of binary blends. In this regard, plots of G' versus ϕ_2 are much more general than plots of J_{eb}^o versus ϕ_2, in describing the effect of blend compositon on fluid elasticity.

We have demonstrated that the semiempirical blending law proposed by Montfort et al.[14,15] is very valuable in predicting the effect of blend composition on the fluid elasticity of binary blends consisting of either nearly monodisperse or polydisperse components, as long as their molecular weights M are greater than the entanglement molecular weight M_e. However, when M is less than M_e for either one or both of the constituent compounds, such as the F90/F008 binary blends of nearly monodisperse polystyrenes (see Table III and Figure 26), the blending law of Montfort et al.,[14,15] applied in this paper, is no longer useful for predicting the effect of blend composition on the linear viscoelastic properties of binary blends.

In this paper we have used the Han-Jhon theory[28] for interpreting the linear viscoelastic behavior of nearly monodisperse polybutadienes with $M \gg M_e$ (see Figs. 5–8). Note that the value of M_e for polybutadiene is 1,800 and that the molecular weight of the polybutadiene 41L, which is the lowest of the

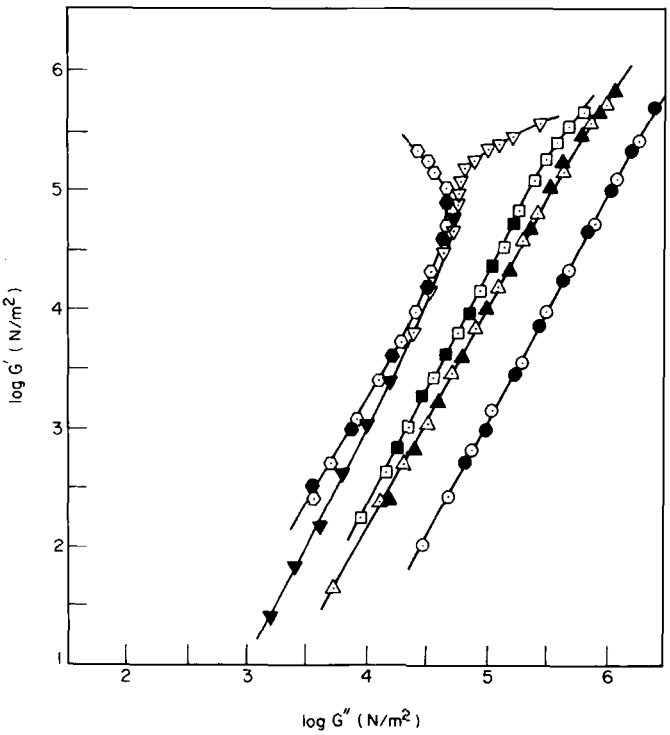

Fig. 47. Log G' vs. log G'' for nearly monodisperse polystyrenes whose molecular weights are given in Table III:[36] (a) F002 at 95°C (⊙) and 102°C (●); (b) F008 at 124°C (△) and 130°C (▲); (c) F018 at 152°C (⊡) and 182°C (■); (d) F11 at 154°C (▽) and 193°C (▼); (e) F90 at 247°C (⊙) and 219°C (●).

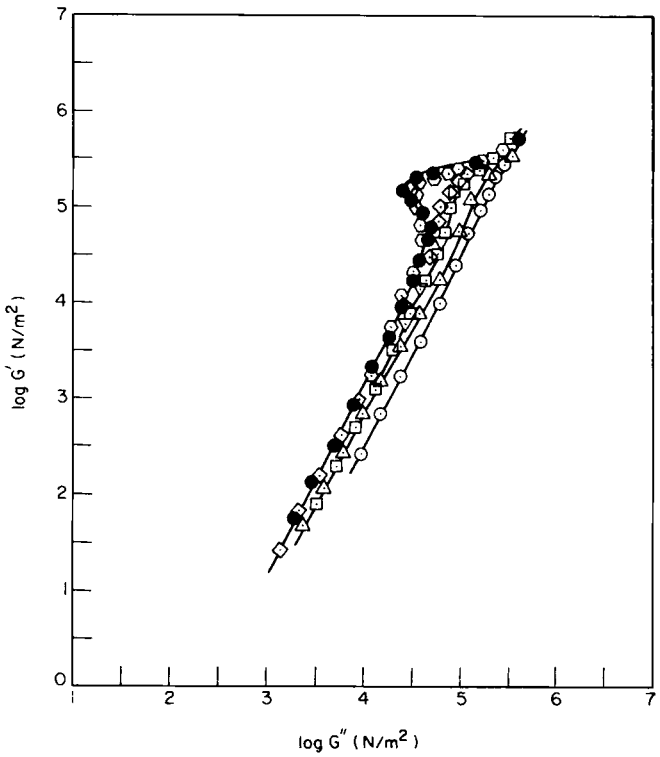

Fig. 48. Log G' vs. log G'' for nearly monodisperse polystyrenes at 167°C, whose molecular weights are given in Table II:[19] (⊙) L23; (△) L39; (⊡) L72; (◇) L89; (▽) L172; (⊙) L315; (●) L427.

three polybutadienes considered above, is 40,700 (see Table I). However, as may be seen in Figures 47 and 48, the experimental data of Montfort and co-workers[17,36] and of Kotaka and co-workers[19,20] for nearly monodisperse polystyrenes showed that log G'–log G'' plots appear to depend upon M even when it is greater than M_e. Note that the value of M_e for polystyrene is about 18,000 ~ 20,000. A close examination of Figures 47 and 48 appears to indicate that log G'–log G'' plots become independent of M when its value reaches several times the value of M_e.

At this juncture, it seems appropriate to mention that according to Graessley[52] J_e^o is constant, with the value

$$J_e^o = 2M_c'/5\rho RT \tag{44}$$

where M_c' is the critical entanglement molecular weight for steady-state compliance. The literature[29,52] suggests that the value of M_c' is about 6 ~ 7 times the value of M_e. In view of the experimental observations made above that the log G'–log G'' plots for nearly monodisperse polystyrenes become independent of molecular weight only when its value becomes several times the value of M_e (see Figs. 47 and 48) and that log G'–log G'' plots describe correctly the dependence of blend composition on G' as the J_e^o does, we

speculate that the critical value of molecular weight at which $\log G'$–$\log G''$ plots become independent of molecular weight may be M_c', rather than M_e. Further experimental data are needed for other monodisperse polymers of different chemical structures, in order to make an unambiguous conclusion on this subject.

I acknowledge gratefully that Dr. M. J. Struglinski has provided me with the data for polybutadienes that were used to prepare Figures 3–20, Professor J. P. Montfort the data for polystyrenes that were used to prepare Figures 24–26 and 47, and Professor T. Kotaka the data for polystyrenes that were used to prepare Figures 21–23 and 48. Without the help received from them, this study would not have been possible.

References

1. K. Ninomiya, *J. Colloid Sci.*, **14**, 49 (1959); **17**, 759 (1962).
2. K. Ninomiya and J. D. Ferry, *J. Colloid Sci.*, **18**, 421 (1963).
3. K. Ninomiya, J. D. Ferry, and Y. Oyanagi, *J. Phys. Chem.*, **67**, 2297 (1963).
4. G. Akovali, *J. Polym. Sci., Part A-2*, **5**, 875 (1967).
5. N. J. Mills and A. Nevin, *J. Polym. Sci., Part A-2*, **9**, 267 (1971).
6. T. Masuda, K. Kitagawa, T. Inoue, and S. Onogi, *Macromolecules*, **3**, 116 (1970).
7. S. Onogi, T. Masuda, N. Toda, and K. Koga, *Polym. J.*, **1**, 542 (1970).
8. D. C. Bogue, T. Masuda, Y. Einaga, and S. Onogi, *Polym. J.*, **1**, 563 (1970).
9. W. M. Prest, *Polym. J.*, **4**, 163 (1973).
10. W. M. Prest and R. S. Porter, *Polym. J.*, **4**, 154 (1973).
11. E. M. Friedman and R. S. Porter, *Trans. Soc. Rheol.*, **19**, 493 (1975).
12. W. W. Graessley, *J. Chem. Phys.*, **54**, 5143 (1971).
13. N. J. Mills, *Eur. Polym. J.*, **5**, 675 (1975).
14. J. P. Montfort, G. Marin, J. Arman, and Ph. Monge, *Polymer*, **19**, 277 (1978).
15. J. P. Montfort, G. Marin, J. Arman, and Ph. Monge, *Rheol. Acta*, **18**, 623 (1979).
16. J. P. Montfort, G. Marin, and Ph. Monge, *Macromolecules*, **17**, 1551 (1984).
17. J. P. Montfort, G. Marin, and Ph. Monge, *Macromolecules*, **19**, 393 (1986).
18. J. P. Montfort, G. Marin, and Ph. Monge, *Macromolecules*, **19**, 1979 (1986).
19. H. Watanabe and T. Kotaka, *Macromolecules*, **17**, 2316 (1984).
20. H. Watanabe, T. Sakamoto, and T. Kotaka, *Macromolecules*, **18**, 1008 (1985).
21. M. J. Struglinski, doctoral dissertation, Northwestern University, Evanston, Illinois, 1984.
22. M. J. Struglinski and W. W. Graessley, *Macromolecules*, **18**, 2630 (1985).
23. W. W. Graessley and M. J. Struglinski, *Macromolecules*, **19**, 1754 (1986).
24. M. Kurata, K. Osaki, Y. Einaga, and T. Sugie, *J. Polym. Sci. Polym. Phys. Ed.*, **12**, 849 (1974).
25. H. K. Chuang and C. D. Han, *J. Appl. Polym. Sci.*, **29**, 2205 (1984).
26. C. D. Han and H. H. Yang, *J. Appl. Polym. Sci.*, **33**, 1199 (1987).
27. C. D. Han and K. W. Lem, *Polym. Eng. Rev.*, **2**, 135 (1983).
28. C. D. Han and M. S. Jhon, *J. Appl. Polym. Sci.*, **32**, 3809 (1986).
29. J. D. Ferry, *Viscoelastic Properties of Polymers*, 3rd ed., Wiley, New York, 1980.
30. M. Doi and S. F. Edwards, *J. Chem. Soc. Faraday Trans. II.*, **74**, 1789, 1802, 1818 (1978).
31. K. Osaki and M. Doi, *Polym. Eng. Rev.*, **4**, 35 (1984).
32. W. E. Rochefort, G. G. Smith, H. Rachapudy, V. R. Raju, and W. W. Graessley, *J. Polym. Sci. Polym. Phys. Ed.*, **17**, 1197 (1979).
33. C. D. Han and H. K. Chuang, *J. Appl. Polym. Sci.*, **30**, 2431 (1985).
34. C. D. Han and H. K. Chuang, *J. Appl. Polym. Sci.*, **30**, 4431 (1985).
35. K. S. Cole and R. H. Cole, *J. Chem. Phys.*, **9**, 341 (1941).
36. J. P. Montfort, personal communication (1986).
37. T. Masuda, K. Kitagawa, and S. Onogi, *Polym. J.*, **1**, 418 (1970).
38. J. S. Noland, H. C. Hsu, R. Saxon, and J. M. Schmitt, in *Multi-component Polymer Systems*, Adv. Chem. Ser. No. 99, Am. Chem. Soc., Washington, D.C., 1971. p. 15.
39. T. Nishi and T. T. Wang, *Macromolecules*, **8**, 909 (1975).
40. T. K. Kwei, H. L. Frisch, W. Radigan, and S. Vogel, *Macromolecules*, **10**, 157 (1977).

41. T. T. Wang and T. Nishi, *Macromolecules*, **10**, 142 (1977).
42. D. J. Stein, R. H. Jung, K. H. Illers, and H. Hendus, *Angew. Makromol. Chem.*, **36**, 89 (1974).
43. L. P. McMaster, in *Copolymer, Polyblends and Composites*, Adv. Chem. Ser. No. 142, Am. Chem. Soc., Washington, D.C., 1975, p. 43.
44. W. A. Kruse, R. G. Kirste, J. Haas, B. J. Schmitt, and D. Stein, *J. Makromol. Chem.*, **177**, 1145 (1976).
45. R. E. Bernstein, C. A. Cruz, D. R. Paul, and J. W. Barlow, *Macromolecules*, **10**, 681 (1977).
46. K. Naito, R. E. Johnson, K. L. Allara, and T. K. Kwei, *Macromolecules*, **11**, 1260 (1978).
47. V. J. McBrierty, D. C. Douglass, and T. K. Kwei, *Macromolecules*, **11**, 1265 (1978).
48. J. V. Koleske, in *Polymer Blends*, edited by D. R. Paul and S. Newman, Chap. 22, Academic Press, New York, 1978.
49. L. P. McMaster, *Macromolecules*, **6**, 760 (1973).
50. C. G. Seefried and J. V. Koleske, *J. Test. Eval.*, **4**, 220 (1976).
51. S. C. Chiu and T. G. Smith, *J. Appl. Polym. Sci.*, **29**, 1781 (1984).
52. W. W. Graessley, *Adv. Polym. Sci.*, **16**, 1 (1974).

Received April 18, 1987
Accepted May 30, 1987